Binding of *Escherichia coli* Primary Replicative Helicase DnaB Protein to Single-Stranded DNA. Long-Range Allosteric Conformational Changes within the Protein Hexamer[†,‡]

Maria J. Jezewska, Ug-Sung Kim, and Wlodzimierz Bujalowski*

Department of Human Biological Chemistry & Genetics, The University of Texas Medical Branch at Galveston, 301 University Boulevard, Galveston, Texas 77555-1053

Received October 2, 1995; Revised Manuscript Received December 13, 1995[⊗]

ABSTRACT: Quantitative analyses of the interactions of the *Escherichia coli* primary replicative helicase DnaB protein with single-stranded ssDNA have been performed using the thermodynamically rigorous fluorescence titration technique. This approach allowed us to obtain absolute stoichiometries of the formed complexes and interaction parameters, without any assumptions about the relationship between the observed signal change and the degree of binding. The analysis of the DnaB helicase interactions with nonfluorescent, unmodified nucleic acids has been performed, using a novel spectroscopic Macromolecular Competition Titration (MCT) method developed in the accompanying paper [Jezewska, M. J., & Bujalowski, W. (1996) *Biochemistry 35*, 2117−2128]. In the presence of the ATP nonhydrolyzable analog AMP-PNP, the DnaB helicase binds polymer ssDNA with a site-size of 20 ± 3 nucleotides per protein hexamer. This site-size is independent of the type of nucleic acid base as well as the salt concentration and type of salt. Direct thermodynamic studies of the polynucleotide and oligomer binding to the DnaB hexamer, as well as the competition studies, show that independently of the type of nucleic acid base, as well as salt concentration and type of salt in solution, the helicase has only a single, strong binding site for DNA. Only this site is used when the protein interacts with polymer ssDNA. Moreover, UV photo-cross-linking experiments with oligonucleotides of different lengths, $dT(pT)_{19}$, $dT(pT)_{55}$, and $dT(pT)_{69}$, suggest that primarily a *single* subunit of the DnaB helicase hexamer is in contact with the ssDNA. In interactions with polymer nucleic acids, the DnaB protein shows preferential intrinsic affinity for poly(dA), characterized in our standard conditions (pH 8.1, 10 °C, 100 mM NaCl, 5 mM $MgCl_2$) by the intrinsic binding constant $K = 6 \pm 2 \times 10^6$ M^{-1}. These affinities are comparable to the affinities of the single-strand binding proteins in the corresponding solution conditions and strongly suggest that the helicase is capable of binding ssDNA without additional facilitating factors. Both the intrinsic affinity and the cooperativity are salt dependent. The formation of the DnaB−ssDNA complex is accompanied by the net release of ∼2 ions, while another net release of ∼2 ions accompanies the cooperative interactions. The data indicate an anion effect on the studied interactions and suggests that the released ions most probably originate from both the protein and the nucleic acid. The presence of a single, strong binding site on the hexamer, built of six chemically identical subunits, the very low site-size of the large helicase−ssDNA complex, and the involvement of a single subunit in contact with the nucleic acid indicate the presence of long-range allosteric interactions in the DnaB helicase which encompass the entire DnaB hexamer. Our sedimentation velocity measurements of the DnaB protein−(AMP-PNP)−5′-fluorescein-$(dT)_{20}$ ternary complex show that the sedimentation coefficient of the complex is $s_{20,w} = 12.3 \pm 0.3$, compared with $s_{20,w} = 10.5 \pm 0.3$ of the free enzyme, indicating large changes in the hydrodynamic properties of the enzyme in the complex. These results provide direct evidence that the DnaB hexamer undergoes dramatic conformational changes which include all six subunits of the enzyme in the ternary complex. Moreover, sedimentation velocity studies of the ternary complex provide direct evidence that the hexamer is the species which binds ss nucleic acid. The significance of these results for a mechanistic model of the functioning of the DnaB helicase in DNA replication is discussed.

The DnaB protein is an essential replication protein in *Escherichia coli* (Kornberg & Baker, 1992) which is involved in both the initiation and elongation stages of DNA replication (Wickner et al., 1973; McMacken et al., 1977; Matson & Kaiser-Rogers, 1990). The protein is the *E. coli* primary replicative helicase, i.e., the factor responsible for unwinding the duplex DNA in front of the replication fork (LeBowitz & McMacken, 1986; Baker et al., 1987; Marians, 1992). The DnaB protein is the only helicase required to reconstitute DNA replication *in vitro* from the chromosomal origin of replication (oriC). In its role as a "mobile replication promoter," DnaB protein binds to ssDNA. The nucleoprotein complex is then specifically recognized by the primase (Arai & Kornberg, 1981b). Multiple activities of the DnaB protein

[†] This work was supported by NIH Grant GM-46679 (to W.B.).

[‡] This work is dedicated to the memory of Dr. Bozena Maria Bujalowska.

[⊗] Abstract published in *Advance ACS Abstracts,* February 1, 1996.

[1] Abbreviations: AMP-PNP, β,γ-imidoadenosine 5′-triphosphate; Tris, tris(hydroxymethyl)aminomethane; EM, electron microscopy.

0006-2960/96/0435-2129$12.00/0

in vitro reflect complex interactions of the helicase with different ingredients in the primosome and in the protein−nucleic acid complexes which are formed at the origins of bacterial and phage DNA replication.

In solution, the native DnaB protein exists as a stable hexamer, composed of six identical subunits (Reha-Krantz & Hurwitz, 1978; Bujalowski et al., 1994). Sedimentation equilibrium, sedimentation velocity, and nucleotide cofactor binding studies show that the DnaB helicase exists as a stable hexamer in a large protein concentration range and magnesium ions play a crucial, structural role in stabilizing the hexameric structure of the enzyme (Bujalowski et al., 1994). Hydrodynamic and EM data indicate that six protomers aggregate with cyclic symmetry in which the protomer−protomer contacts are limited to only two neighboring subunits (Bujalowski et al., 1994; San Martin et al., 1995).

The binding or the binding and hydrolysis of ATP is the key element regulating DnaB protein activities (Kornberg & Baker, 1992; Arai & Kornberg, 1981a,b; LeBowitz & McMacken, 1986). Quantitative studies of the nucleotide binding to the DnaB helicase have established that the hexamer has six nucleotide binding sites, presumably one on each protomer (Arai & Kornberg, 1981b; Bujalowski & Klonowska, 1993). On the basis of thermodynamically rigorous fluorescence titrations, we have determined that the binding process is biphasic which results from the negative cooperative interactions among binding sites (Bujalowski & Klonowska, 1993, 1994a,b).

In vivo functions of the DnaB helicase are related to the ability of the protein to interact with ss and dsDNA under ATP/ADP switch control (Arai & Kornberg, 1981b). Recently, we obtained the very first estimation of the stoichiometry of the DnaB helicase−ssDNA complex and the mechanism of the binding (Bujalowski & Jezewska, 1995). Using the quantitative fluorescence titration method, we determined that the DnaB helicase binds an etheno derivative of poly(dA), poly(dϵA), with a stoichiometry of 20 ± 3 nucleotides per DnaB hexamer. Although the importance of understanding the DnaB protein interactions with nucleic acid has been recognized, little is known about the stoichiometry (site-size) of the DnaB complexes with different ss and dsDNA, the base effect, the sequence specificity, the solution conditions on the intrinsic affinity, the cooperativity of the binding process, and the structure of the complexes. Knowledge of the stoichiometry and structure of the helicase−nucleic acid complex and the mechanism of binding is a prerequisite for formulating any model of the mechanism of enzyme functioning in DNA replication.

In this communication, we report extensive, quantitative analyses of the interactions of the DnaB helicase with ssDNA, using the thermodynamically rigorous fluorescence titration techniques. We present direct evidence that in the presence of the ATP nonhydrolyzable analog, AMP-PNP, the DnaB helicase binds the polymer ssDNA with a site-size of 20 ± 3 nucleotides per DnaB hexamer, independent of the type of nucleic acid base and solution conditions. Photo-cross-linking experiments with ssDNA oligomers of different lengths, $dT(pT)_{19}$, $dT(pT)_{55}$, and $dT(pT)_{69}$, indicate that only a single subunit of the DnaB hexamer is primarily in contact with ssDNA in the protein−DNA complex, even in the presence of excess ssDNA. The intrinsic affinity of the DnaB helicase shows a preference for poly(dA) and, in corresponding solution conditions, is comparable with the intrinsic affinity of single-strand binding proteins (SSB).

Sedimentation velocity measurements reveal that the DnaB hexamer undergoes dramatic conformational changes upon forming a ternary complex, DnaB−(AMP-PNP)−ssDNA and provide direct evidence of the presence of long-range allosteric interactions in the hexamer encompassing all six subunits of the enzyme.

MATERIALS AND METHODS

Reagents and Buffers. All solutions were made with distilled and deionized >18 MΩ (Milli-Q Plus) water. All chemicals were reagent grade. Buffer T2 is 50 mM Tris adjusted to pH 8.1 with HCl, 5 mM $MgCl_2$, 10% glycerol.

DnaB Protein. The *E. coli* DnaB protein was purified as previously described by us (Bujalowski & Klonowska, 1993, 1994a; Bujalowski et al., 1994). The concentration of the protein was spectrophotometrically determined using extinction coefficient $\epsilon_{280} = 1.85 \times 10^5$ cm^{-1} M^{-1} (Hexamer) (Bujalowski et al., 1994).

Nucleic Acids. Oligomers $dA(pA)_{19}$, $dA(pA)_{39}$, $dT(pT)_{19}$, $dT(pT)_{55}$, $dT(pT)_{69}$, $dC(pC)_{20}$ and homopolymers poly(dA), poly(dC), and poly(dT) were purchased from Midland Certified Reagents (Midland, TX) and Sigma. Poly(A), poly(U), and poly(C) were from Fluka. The etheno derivatives of nucleic acids were obtained by modification with chloroacetaldehyde (Secrist et al., 1972). Oligomer $dT(pT)_{19}$, labeled at the 5′-end with fluorescein, has been synthesized using fluorescein phosphoramidate (Glen Research). The concentrations of the labeled oligomer was determined at 492 nm (pH 9) and at 260 nm using extinction coefficients 7.1×10^4 M^{-1} cm^{-1} at 492 nm and 1.76×10^5 M^{-1} cm^{-1} at 260 nm (pH 8.1). The concentrations of polynucleotides were determined spectrophotometrically using the following extinction coefficients (Nucleotide): 10×10^3 M^{-1} cm^{-1}, poly(dA) at 257 nm; 10.3×10^3 M^{-1} cm^{-1}, poly(A) at 260 nm; 8.1×10^3 M^{-1} cm^{-1}, poly(dT) at 260 nm; 7.2×10^3 M^{-1} cm^{-1}, poly(dC) at 270 nm; 6.5×10^3 M^{-1} cm^{-1}, poly(C) at 267 nm; 9.2×10^3 M^{-1} cm^{-1}, poly(U) at 260 nm; and 9.4×10^3 M^{-1} cm^{-1}, poly(dI) at 260 nm (Kowalczykowski et al., 1981). The concentration of the etheno derivative of nucleic acids was determined using extinction coefficient 3700 M^{-1} cm^{-1} (Nucleotide) at 257 nm (Ledneva, et al., 1977).

Photo-Cross-Linking Experiments. Oligomers $dT(pT)_{19}$, $dT(pT)_{55}$, and $dT(pT)_{69}$ have been labeled at the 5′-end with [^{32}P] using polynucleotide kinase according to the protocol described by Sambrook et al. (1989). The labeled ssDNAs were mixed with the DnaB helicase in buffer T2 (pH 8.1, 20 °C) containing 1 mM AMP-PNP and different NaCl concentrations (see below). After 1 h incubation at 10 °C the samples (total volume 10 μL) were placed on Parafilm, immersed in a 10 °C water bath, and irradiated for 30 min, at a distance of 11 cm, using a mineral lamp (model UVG-11) with a maximum output of 254 nm. After irradiation, the samples were loaded on 8% SDS polyacrylamide gel and electrophoresis was performed at a constant voltage of 230 V. The gels were stained with Coomassie Brilliant Blue, dried, and autoradiographed.

Sedimentation Velocity Measurements. Sedimentation velocity experiments were performed using a Spinco model E analytical centrifuge. The analysis of the sedimentation

runs was performed, as previously described by us (Bujalowski et al., 1994). The reported values of sedimentation coefficients were corrected to standard conditions, $s_{20,w}$, for solvent density and viscosity (Tanford, 1961).

Fluorescence Measurements. All steady-state fluorescence titrations were performed using the SLM-AMINCO 48000S spectrofluorimeter. The binding was followed by monitoring the fluorescence of the etheno derivative of poly(dA), poly(dϵA), (λ_{ex} = 325 nm, λ_{em} = 410 nm). All titration points were corrected for dilution and, if necessary, for inner filter effects using the following formula (Lakowicz, 1983)

$$F_{icor} = (F_i - B_i)\left(\frac{V_i}{V_o}\right) \times 10^{0.5b(A_{i_{\lambda ex}})} \quad (1)$$

where F_{icor} is the corrected value of the fluorescence intensity at a given point of titration i, F_i is the experimentally measured fluorescence intensity, B_i is the background, V_i is the volume of the sample at a given titration point, V_o is the initial volume of the sample, b is the total length of the optical path in the cuvette expressed in cm, $A_{i_{\lambda ex}}$ is the absorbance of the sample at the excitation wavelength. Computer fits were performed using KaleidaGraph software (Synergy Software, PA) and Mathematica (Wolfram Research, IL).

The relative fluorescence increase of the nucleic acid, ΔF, upon binding the DnaB protein is defined by

$$\Delta F = \frac{(F_i - F_o)}{F_o} \quad (2)$$

where F_i is the fluorescence of the nucleic acid solution at a given titration point "i" and F_o is the initial value of the fluorescence of the same solution.

Determination of Rigorous Thermodynamic Binding Isotherms and Absolute Stoichiometries of the DnaB Helicase−ssDNA Complexes. In this work, we followed the binding of the DnaB protein to polymer and oligomer ssDNAs, by monitoring the fluorescence increase, ΔF_{obs}, of their etheno derivatives upon the complex formation. To obtain absolute estimates of the average degree of binding of the protein per nucleotide, $\sum\nu_i$ (binding density), and the free protein concentration, P_F, we applied a procedure described in detail in the accompanying paper. The experimentally observed ΔF_{obs} has a contribution from each different possible "i" complexes of the DnaB hexamer with ssDNA. Thus, the observed fluorescence increase is functionally related to $\sum\nu_i$ by eq 3 (Bujalowski & Klonowska, 1993; Bujalowski & Jezewska, 1995)

$$\Delta F_{obs} = \sum \nu_i \Delta F_{i_{max}} \quad (3)$$

where $\Delta F_{i_{max}}$ is the molecular parameter characterizing the maximum fluorescence increase of the nucleic acid with the DnaB protein bound in complex "i". The same value of ΔF_{obs}, obtained at two different total nucleic acid concentrations, N_{T_1} and N_{T_2}, indicates the same physical state of the nucleic acid, i.e., the degree of binding, $\sum\nu_i$, and the free DnaB protein concentration, P_F, must be the same. The value of $\sum\nu_i$ and P_F is then related to the total protein concentrations, P_{T_1} and P_{T_2}, and the total nucleic acid concentrations, N_{T_1} and N_{T_2}, at the same value of ΔF_{obs}, by

$$\sum \nu_i = \frac{(P_{T_2} - P_{T_1})}{(N_{T_2} - N_{T_1})} \quad (4)$$

$$P_F = P_{T_x} - (\sum \nu_i) N_{T_x} \quad (5)$$

where x = 1 or 2 (Bujalowski & Klonowska, 1993).

Determination of the Absolute Stoichiometry of the DnaB Protein−Unmodified Nucleic Acid Complex Using the MCT Method. Determination of the site-size and the interaction parameters for the DnaB helicase−unmodified nucleic acid complex has been performed using the MCT method described in the accompanying paper. Briefly, if the fluorescent reference macromolecule (nucleic acid) at total concentration, N_{T_R}, is titrated with the protein in the presence of a competing nonfluorescent nucleic acid of total concentration N_{1_S}, then the total concentration of the protein, P_{T_1}, at which a given fluorescence change, ΔF_i, is observed is described by

$$P_{T_1} = (\sum \nu_i)_S N_{1_S} + (\sum \nu_i)_R N_{T_R} + P_F \quad (6a)$$

where $(\sum\nu_i)_R$, $(\sum\nu_i)_S$, and P_F are the binding density of the protein on the reference fluorescent nucleic acid, the binding density of the protein on the nonfluorescent, competing nucleic acid, and the free protein concentration, respectively. The total concentration of the protein, P_{T_2}, at which the same ΔF_i is observed at the same N_{T_R}, but with a different total concentration of competing nucleic acid, N_{2_S}, is described by

$$P_{T_2} = (\sum \nu_i)_S N_{2_S} + (\sum \nu_i)_R N_{T_R} + P_F \quad (6b)$$

Subtracting eq 6a from eq 6b and rearranging provides eq 7, which allows us to determine the absolute binding density of the protein on the competing nonfluorescent nucleic acid lattice (M. J. Jezewska and W. Bujalowski, accompanying paper).

$$(\sum \nu_i)_S = \frac{(P_{T_2} - P_{T_1})}{(N_{2_S} - N_{1_S})} \quad (7)$$

Analysis of the DnaB Hexamer−Polymer ssDNA Binding Isotherm. McGhee and von Hippel (1974) derived two explicit equations for noncooperative and cooperative binding of a large ligand to a one-dimensional homogeneous, infinite lattice which takes into account the potential overlap between binding sites. Previously, we derived a single, generalized equation for the McGhee−von Hippel model which can be applied to both cooperative and noncooperative binding (Bujalowski et al., 1989). The binding density, $\sum\nu_i$, is described using the generalized equation by the following expression:

$$\sum \nu_i = K(1 - n\sum \nu_i) \times \left\{\frac{[2\omega(1 - n\sum \nu_i)]}{[(2\omega - 1)(1 - n\sum \nu_i) + \sum \nu_i + R]}\right\}^{(n-1)} \left\{\frac{[1 - (n+1)\sum \nu_i + R]}{2(n - \sum \nu_i)}\right\}^2 P_F \quad (8)$$

where K is the intrinsic binding constant, n is the number of

nucleotides covered by the protein in the complex (site-size), ω is the parameter characterizing cooperativity, and $R = \{[1 - (n + 1)\sum\nu_i]^2 + 4\omega\sum\nu_i(1 - n\sum\nu_i)\}^{0.5}$.

If the fluorescence increase of the nucleic acid is strictly proportional to the binding density of the protein, $\sum\nu_i$, then the fractional saturation of the lattice is equal the fractional signal change as defined by

$$\frac{N_b}{N_T} = \frac{\Delta F_{obs}}{\Delta F_{max}} \tag{9}$$

where N_b is the concentration of a bound nucleic acid (Nucleotide), N_T is the total concentration of the nucleic acid, ΔF_{obs} is the observed signal at a given titration point *i*, and ΔF_{max} is the maximum fluorescence increase of the nucleic acid at saturation with the protein. N_b can be defined in terms of the site-size, *n*, and the concentration of the bound protein, P_b, as

$$N_b = nP_b = n(\sum\nu_i)N_T \tag{10}$$

Introducing eq 10 into eq 9 and rearranging provides the expression for the observed fluorescence increase of the nucleic acid titrated with the DnaB protein as

$$\Delta F_{obs} = \Delta F_{max} n(\sum\nu_i) \tag{11}$$

where $\sum\nu_i$ is defined by the generalized McGhee-von Hippel equation, eq 8. Binding of the DnaB helicase to poly(dϵA) has been analyzed using eqs 8 and 11.

Analysis of the Lattice Competition Titration Curves. The analysis of the titration curves of the fluorescent nucleic acid (etheno derivatives) in the presence of a competing non-fluorescent, unmodified nucleic acid was performed using the combined application of the McGhee-von Hippel model and the combinatorial theory of Epstein (1978) and is described in detail in the accompanying paper.

Statistical Thermodynamic Model of the DnaB Helicase Hexamer Binding to 40-mer. Binding studies presented below show that, at saturation, a single molecule of dϵA-(pϵA)$_{39}$ can accommodate two DnaB hexamers independently of solution conditions. The partition function, *Z*, for the DnaB hexamer−40-mer system, which accounts for the potential overlap of the binding sites' cooperative interactions between bound protein molecules, is described by

$$Z = 1 + (N - n + 1)K_{40}P_F + \omega K_{40}^2 P_F^2 \tag{13}$$

where *N* is the total number of residues in the ss nucleic acid oligomer, *n* is the site-size of the hexamer−ssDNA complex, K_{40} is the intrinsic binding constant, and ω is the parameter characterizing the cooperative interactions between the two bound hexamers. The average number of DnaB hexamers bound per 40-mer, *q*, is then defined by the standard statistical thermodynamic expression $q = \partial \ln Z/\partial \ln P_F$ (Hill, 1985).

$$q = \frac{(N - n + 1)K_{40}P_F + 2\omega K_{40}^2 P_F^2}{1 + (N - n + 1)K_{40}P_F + \omega K_{40}^2 P_F^2} \tag{13}$$

The relative increase of the fluorescence of the dϵA(pϵA)$_{39}$, ΔF_1, upon binding the first DnaB hexamer differs from the relative fluorescence increase, ΔF_2, observed upon binding of the second hexamer (Bujalowski & Jezewska, 1995). The experimentally monitored relative increase of the nucleic acid fluorescence, ΔF_{obs}, is then defined in terms of ΔF_1, ΔF_2, intrinsic binding constant K_{40}, and cooperativity parameter ω as

$$\Delta F_{obs} = \frac{[(\Delta F_1)(N - n + 1)K_{40}^2 P_F + (\Delta F_1 + \Delta F_2)\omega K_{40}^2 P_F^2]}{[Z]} \tag{14}$$

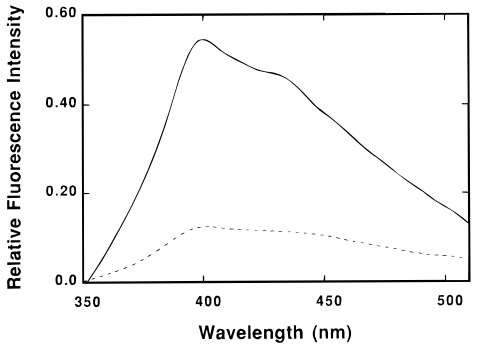

FIGURE 1: Corrected fluorescence emission spectra ($\lambda_{ex} = 325$ nm) of dϵA(pϵA)$_{39}$ [4.9×10^{-7} M (Oligomer)] in buffer T2 (pH 8.1, 10 °C) containing 100 mM NaCl and 1 mM AMP-PNP in the absence (- - -) and presence (—) of the DnaB helicase. The DnaB protein concentration is 3.4×10^{-5} M (Hexamer).

RESULTS

Determination of the Absolute Stoichiometry of DnaB Hexamer−ssDNA Complexes Using ssDNA Etheno Derivatives. In the presence of an ATP nonhydrolyzable analog, AMP-PNP, binding of the DnaB helicase to poly(dϵA) causes a strong increase of the fluorescence of the nucleic acid (Bujalowski & Jezewska, 1995). Corrected fluorescence emission spectra ($\lambda_{ex} = 325$ nm) of dϵA(pϵA)$_{39}$ in the absence and presence of the saturating concentration of the DnaB helicase in buffer T2 (pH 8.1, 10 °C) containing 100 mM NaCl and 1 mM AMP-PNP, are shown in Figure 1. This oligomer has been selected because it accommodates two DnaB hexamers, hence, introducing both intrinsic and cooperative interactions, and can be practically completely saturated with the DnaB protein in the experimentally accessible protein concentration range. The emission maximum of the free nucleic acid is located at 400 nm. Binding of the DnaB helicase enhances the fluorescence intensity ~4-fold without changing the location of the maximum or the shape of the fluorescence spectrum. Because at 325 nm (excitation wavelength) only the etheno adenine is excited, the observed fluorescence increase must result from the increase of the nucleic acid quantum yield. It should be noted, that incorporation of ϵA into the polymer induces an 8−10-fold quenching of the ϵA fluorescence, as compared to the free mononucleotide (Tolman et al., 1974). Thus, the strong increase of the nucleic acid fluorescence, when bound to the DnaB helicase, indicates that some of the quenching processes have been removed in the complex with the helicase (see Discussion).

The dramatic enhancement of the ssDNA etheno derivative provides an excellent signal to monitor the DnaB−ssDNA interactions and to perform high-resolution measurements of the stoichiometry and mechanism of the helicase−ssDNA

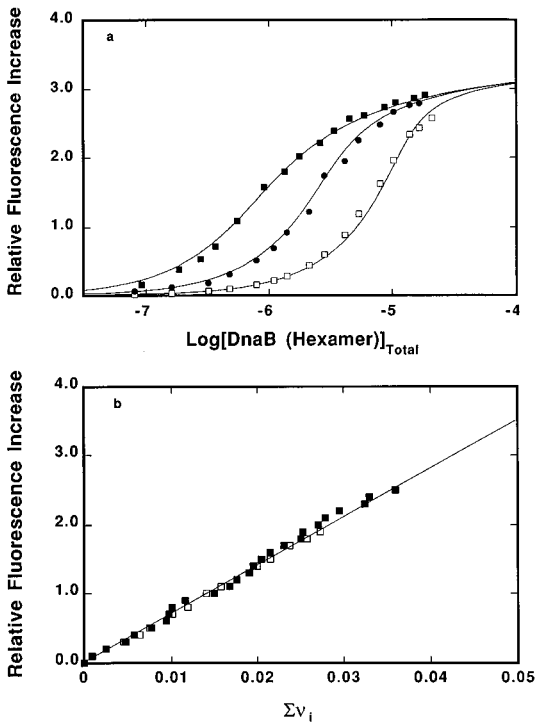

FIGURE 2: a. Fluorescence titrations of poly(dϵA) with the DnaB protein in buffer T2 (pH 8.1, 10 °C) containing 100 mM NaCl and 1 mM AMP-PNP, at three different nucleic acid concentrations: (■) 2.0×10^{-5} M; (●) 8.4×10^{-5} M; (□) 3.2×10^{-4} M (Nucleotide). Solid lines are computer fits of the binding isotherms, using the generalized McGhee−von Hippel equation (eqs 8 and 11), with intrinsic binding constant $K = 1.3 \times 10^5$ M^{-1}, cooperativity parameter $\omega = 3.5$, and $\Delta F_{max} = 3.5$. b. Dependence of the relative increase of the poly(dϵA) fluorescence upon the average binding density, $\sum\nu_i$, of the DnaB helicase hexamer in buffer T2 (pH 8.1, 10 °C) containing 1 mM AMP-PNP and (■) 100 mM NaCl; (□) 196 mM NaCl. The absolute value of $\sum\nu_i$ has been determined using the thermodynamically rigorous approach described in Materials and Methods.

complex formation. Fluorescence titrations of poly(dϵA) with the DnaB helicase, at three different nucleic acid concentrations, in buffer T2 (pH 8.1, 10 °C) containing 100 mM NaCl and 1 mM AMP-PNP, are shown in Figure 2a. As the nucleic acid concentration increases, a given relative fluorescence increase is reached at higher DnaB protein concentrations. The selected nucleic acid concentrations provide separation of binding isotherms up to the relative fluorescence increase of ∼2.7. To obtain thermodynamically rigorous binding parameters, independent of any assumption about the relationship between the observed signal and the degree of binding, $\sum\nu_i$, the fluorescence titrations curves shown in Figure 2a have been analyzed, using the approach outlined in Materials and Methods and in the accompanying paper. Figure 2b shows the dependence of the observed relative fluorescence increase as a function of the average binding density, $\sum\nu_i$, of the DnaB helicase (closed squares). The value of $\sum\nu_i$ could be determined up to ∼0.033 (i.e., up to ∼30 nucleotides per DnaB helicase hexamer). The plot is linear indicating that in the studied binding density range there is a very similar enhancement of the nucleic acid fluorescence upon the binding of the DnaB protein. However, the linearity in the whole range of the binding density is not preserved in the DnaB protein interaction with shorter lattices (see below).

At higher binding density ranges, binding of a large ligand to a one-dimensional lattice is characterized by a large negative entropy factor which results from difficulties in the formation of a gap of free nucleotide residues large enough to accommodate the ligand (McGhee & von Hippel, 1974). In order to obtain complete saturation of the nucleic acid lattice, extremely high concentrations of the ligand would be required. To overcome this problem, we estimated the maximum relative fluorescence increase of poly(dϵA), using a number of dϵA(pϵA)$_{N-1}$ oligomers, with the length of the oligomers ranging from 20 to 60 residues in a range of studied solution conditions [Bujalowski and Jezewska (1995) and see below]. Using these short lattices, the gap problem has been greatly reduced or eliminated. Moreover, full saturation can be reached in an experimentally accessible protein concentration range. Within experimental accuracy, the relative increase of the fluorescence of the studied ethenoadenosine oligomers in buffer T2 (pH 8.1, 10 °C) containing 100 mM NaCl was constant, independent of the length of the oligonucleotide, and equal to 3.5 ± 0.2. Thus, the estimated value of the maximum fluorescence increase of poly(dϵA) upon binding to DnaB is 3.5 ± 0.2. Extrapolation to $\Delta F_{max} = 3.5 \pm 0.2$ gives the maximum value of $\sum\nu_i = 0.05 \pm 0.008$. Analogous experiments at lower and higher salt concentrations provide the same linear dependence of the observed signal as a function of the binding density.

Using the MCT method described in the accompanying paper, the site-size of the DnaB hexamer complex with unmodified polynucleotides poly(dA), poly(dT), poly(dC), and poly(dI) has also been determined. Fluorescence titrations of the poly(dϵA) sample in the presence of two different concentrations of poly(dC), but at the same poly(dϵA) concentration in buffer T2 (pH 8.1, 10 °C) containing 100 mM NaCl and 1 mM AMP-PNP are shown in Figure 3a. In this competition experiment, the binding of the protein to the "marker" fluorescent polynucleotide has been monitored. In the presence of the competing nonfluorescent nucleic acid, the binding isotherm is shifted toward higher protein concentrations due to the simultaneous binding of the protein to the competing, unmodified polynucleotide. On the other hand, at the same value of the fluorescence increase of poly(dϵA), independently of the concentration of the competing polynucleotide, the physical state of the fluorescent nucleic acid must be the same, i.e., the values of $(\sum\nu_i)_R$ and the free protein concentration $[DnaB]_F$ must be the same (M. J. Jezewska and W. Bujalowski, accompanying paper). The binding density of the protein, on the competing, unmodified ssDNA, $(\sum\nu_i)_S$, is also a sole, unique function of the $[DnaB]_F$. Therefore, at a given value of fluorescence increase, the value of $(\sum\nu_i)_S$ must be the same, independent of the concentration of unmodified nucleic acid. The binding density, $(\sum\nu_i)_S$, can then be obtained using eq 7 (Materials and Methods, accompanying paper). The dependence of the observed fluorescence increase of poly(dϵA) upon the binding density, $(\sum\nu_i)_S$, of the DnaB protein−poly(dC) complex is shown in Figure 3b. The highest measured value of $(\sum\nu_i)_S$ is ∼0.035 at the relative fluorescence increase $\Delta F \approx 2.5$, corresponding with 28 nucleotide residues per DnaB hexamer. Extrapolation to the maximum value of the relative fluorescence increase (3.5) provides $(\sum\nu_i)_S = 0.05 \pm 0.01$ (M. J. Jezewska and W. Bujalowski, accompanying paper). Using the MCT method, the same site-size has been determined in competition experiments with poly(dT), poly(dA), and poly(dI), indicating that the stoichiometry of the DnaB hexamer complex with ssDNA is base independent (Table 1).

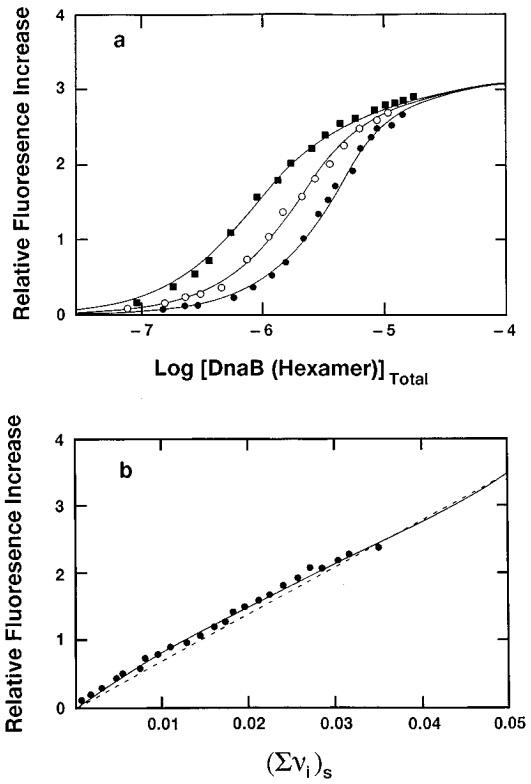

FIGURE 3: a. Fluorescence titrations of poly(dϵA) with the DnaB protein in buffer T2 (pH 8.1, 10 °C) containing 100 mM NaCl and 1 mM AMP-PNP, in the presence of two different concentrations of poly(dC): (○) 5.1×10^{-5} M; (●) 1.26×10^{-4} M (Nucleotide) (lattice competition titrations). The titration of poly(dϵA) alone in the same buffer conditions is also included (■). Solid lines are computer fits of the binding isotherms using the generalized McGhee-von Hippel equation (eqs 8 and 11) to describe the binding of the helicase to poly(dϵA), with intrinsic binding constant $K = 1.3 \times 10^5$ M^{-1}, cooperativity parameter $\omega = 3.5$, and $\Delta F_{max} = 3.5$. Binding of the DnaB protein to poly(dC) has been described by the Epstein combinatorial theory, using intrinsic binding constant $K = 1 \times 10^5$ M^{-1} and cooperativity parameter $\omega = 5$ (M. J. Jezewska and W. Bujalowski, accompanying paper). b. Dependence of the relative increase of the poly(dϵA) fluorescence upon the average binding density, $(\Sigma\nu_i)_S$, of the DnaB helicase hexamer on the competing nucleic acid lattice, poly(dC) (●) (see text for details). The absolute value of $(\Sigma\nu_i)_S$ for the binding of the DnaB helicase on poly(dC) has been determined, using the MCT method (M. J. Jezewska and W. Bujalowski, accompanying paper). The solid line is the computer simulation of the dependence of the observed fluorescence increase upon the average binding density, $(\Sigma\nu_i)_S$ of the DnaB helicase hexamer on the poly(dC) using the independently determined binding constants for both the DnaB−poly(dϵA) and DnaB−poly(dC) complexes in the same solution conditions (Table 2). The dependence of the relative fluorescence increase of poly(dϵA) upon the binding density, $(\Sigma\nu_i)_R$, of the DnaB helicase on poly(dϵA), in the same buffer conditions, is also included (dashed, straight line).

The stoichiometry of the DnaB hexamer−ssDNA complex, at different salt concentrations, has been further examined using short ssDNA oligomers, dϵA(pϵA)$_{39}$, and dϵA(pϵA)$_{19}$. Fluorescence titrations of dϵA(pϵA)$_{39}$ with the DnaB helicase in buffer T2 (pH 8.1, 10 °C) containing 100 mM NaCl and 1 mM AMP-PNP, at two different nucleic acid concentrations, are shown in Figure 4a. The two oligomer concentrations differ by a factor of ∼7, providing a distinct separation of the binding isotherms up to 80% of the maximum saturation. The observed maximum fluorescence increase of dϵA(pϵA)$_{39}$ fluorescence is 3.5 ± 0.2. The binding process is clearly biphasic with the high-affinity step characterized by the higher fluorescence increase (∼2.2).

The dependence of the observed fluorescence increase upon the average number of DnaB hexamers bound per 40 mer at different NaCl concentrations is shown in Figure 4b. In contrast to poly(dϵA), the plot is nonlinear and the binding of the first hexamer is accompanied by a larger fluorescence increase ($\Delta F_1 = 2.2$, eq 14). In the presence of 100 mM NaCl, the separation of the binding isotherms allowed us to determine the degree of binding, q, up to ∼1.6 hexamers per 40-mer (closed squares). Extrapolation to $\Delta F_{max} = 3.5$ shows that two DnaB hexamers bind to a single dϵA(pϵA)$_{39}$ molecule which is in excellent agreement with the stoichiometry of the DnaB−ssDNA complex determined using both modified and unmodified ssDNA. The solid line is the computer simulation of the relative fluorescence increase, as a function of the average number of DnaB hexamers bound to 40-mer, using $n = 20$, and the independently determined binding parameters $K_{40} = 9 \times 10^6$ M^{-1} and $\omega = 0.03$ (see below). Due to the lower affinity, the average number of DnaB hexamers bound per dϵA(pϵA)$_{39}$ in the presence of 196 mM NaCl could only be determined up to $q \approx 1.2$ (opened squares). Nevertheless, both plots superimpose very well in the accessible range of q, indicating that the stoichiometry of the DnaB−dϵA(pϵA)$_{39}$ complex is independent of salt concentration.

Binding of ssDNA 20-mer to the DnaB Helicase. Fluorescence titrations of dϵA(pϵA)$_{19}$ with the DnaB helicase in buffer T2 (pH 8.1, 10 °C) containing 100 mM NaCl and 1 mM AMP-PNP, at four different nucleic acid concentrations are shown in Figure 5a. At each 20 mer concentration studied, the binding process is monophasic and the maximum increase of the nucleic acid fluorescence is 3.4 ± 0.2. Separation of the binding isotherms allowed us to determine the stoichiometry of the DnaB−20-mer complex up to 90% of the maximum saturation. The dependence of the observed relative fluorescence increase upon the average degree of binding of the DnaB protein on dϵA(pϵA)$_{19}$ is shown in Figure 5b. The plots are strictly linear and show that at saturation only one 20-mer molecule binds to a single DnaB hexamer.

The stoichiometry of the DnaB hexamer−20-mer complex, with different nonfluorescent oligomers, has been determined using the MCT method (M. J. Jezewska and W. Bujalowski, accompanying paper). Because the affinities of 20-mers to the DnaB protein are very high (Table 2), the determination of stoichiometries has been performed at elevated salt concentrations in order to obtain also more accurate estimates of the binding constants. Figure 6a shows the representative fluorescence titrations of dϵA(pϵA)$_{19}$ with the DnaB protein in buffer T2 (pH 8.1, 10 °C) containing 293 mM NaCl and 1 mM AMP-PNP in the presence of two different dC(pC)$_{19}$ concentrations. A significant shift of the binding isotherm, with increasing dC(pC)$_{19}$ concentrations, indicates strong competition between dϵA(pϵA)$_{19}$ and dC(pC)$_{19}$ for the DnaB hexamer. The dependence of the observed fluorescence increase upon the average number of DnaB hexamers bound per single dC(pC)$_{19}$ molecule is shown in Figure 6b. Due to the high affinity of DnaB toward dC(pC)$_{19}$, even at the low value of the fluorescence increase of dϵA(pϵA)$_{19}$ there is substantial binding of DnaB to the cytidine oligomer (Table 2). At $\Delta F \approx 1.1$, the plot reaches the stoichiometry of 1 ± 0.15 DnaB hexamer bound per dC(pC)$_{19}$ molecule. An additional increase of the DnaB concentration does not

Table 1: Thermodynamic Parameters, the Number of Covered Nucleotides by Protein Molecule (Site-Size) n, the Intrinsic Binding Constant K, and the Cooperativity Parameter ω for Interactions of DnaB Helicase with Single-Stranded Polynucleotides and 40-mer dϵA(pϵA)$_{39}$ in Buffer T2 (pH 8.1, 10 °C) Containing 100 mM NaCl and 1 mM AMP-PNP

	poly(dϵA)	poly(dA)	poly(dT)	poly(dI)	poly(dC)	poly(A)	poly(U)	poly(C)	dϵA(pϵA)$_{39}$
n	20 ± 3	20 ± 3	20 ± 3	20 ± 3	20 ± 3	ND	ND	ND	20 ± 3
K (M^{-1})	$(1.3 \pm 0.3) \times 10^5$	$(6 \pm 2) \times 10^6$	$(1 \pm 0.5) \times 10^4$	$(5 \pm 3) \times 10^4$	$(1 \pm 0.3) \times 10^5$	$(6.5 \pm 2) \times 10^3$	$(4 \pm 1) \times 10^4$	$\sim 10^2$	$(9 \pm 2) \times 10^6$
ω	3.5 ± 1	6 ± 3	≤ 10	≤ 10	5 ± 3	≤ 5	≤ 5	ND	0.03 ± 0.01

[a] ND, not determined.

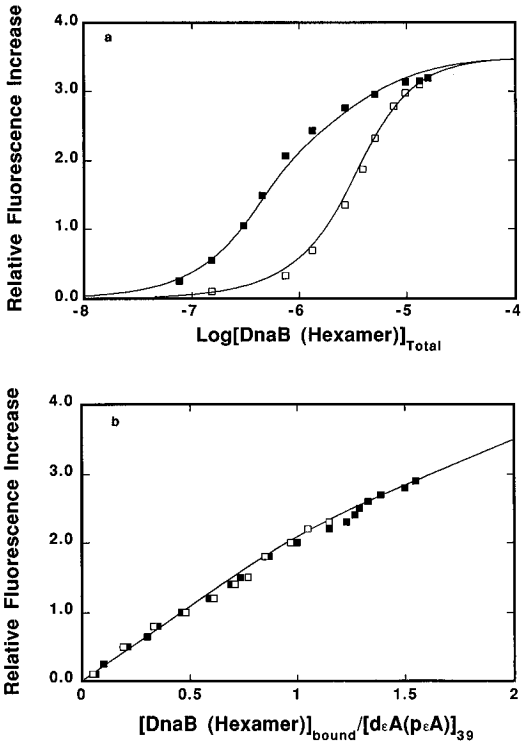

FIGURE 4: a. Fluorescence titrations of dϵA(pϵA)$_{39}$ with the DnaB helicase monitored by the relative increase of the nucleic acid fluorescence in buffer T2 (pH 8.1, 10 °C) containing 100 mM NaCl and 1 mM AMP-PNP at two different nucleic acid concentrations (Oligomer): (■) 4.9×10^{-7} M; (□) 3.4×10^{-6} M. Solid lines are computer fits of the binding isotherms using the equation for the large ligand binding to the short lattice (see eq 14) with intrinsic binding constant, $K_{40} = 9 \times 10^6$ M^{-1}, $n = 20$, cooperativity parameter $\omega = 0.03$, $\Delta F_1 = 2.2$, and $\Delta F_2 = 1.3$. b. Dependence of the increase of the dϵA(pϵA)$_{39}$ fluorescence upon the average number of DnaB helicase hexamers bound per oligomer (q) in different salt concentrations: (■) 100 mM NaCl; (□) 196 mM NaCl. The absolute value of q has been determined using the thermodynamically rigorous approach described in Materials and Methods. The solid line is the computer simulation of the dependence of ΔF_{obs} upon q using independently determined binding and spectroscopic parameters (eq 14), $K_{40} = 9 \times 10^6$ M^{-1}, cooperativity parameter $\omega = 0.03$, $\Delta F_1 = 2.2$, and $\Delta F_2 = 1.3$ for the binding of the DnaB helicase to dϵA(pϵA)$_{39}$ in buffer T2 (pH 8.1, 10 °C) containing 100 mM NaCl and 1 mM AMP-PNP.

change the determined stoichiometry of the DnaB−dC(pC)$_{19}$ complex. The observed increase of the dϵA(pϵA)$_{19}$ fluorescence results from continuing the binding of the DnaB protein to the etheno oligomer, after the saturation of dC(pC)$_{19}$ has been reached. The solid line in Figure 6b is the computer simulation of the dependence of the observed fluorescence increase upon the average number of DnaB hexamers bound per dC(pC)$_{19}$ using the independently determined binding constants for both the DnaB−dϵA(pϵA)$_{19}$ and DnaB−dC(pC)$_{19}$ complexes in the same solution conditions (Table 2).

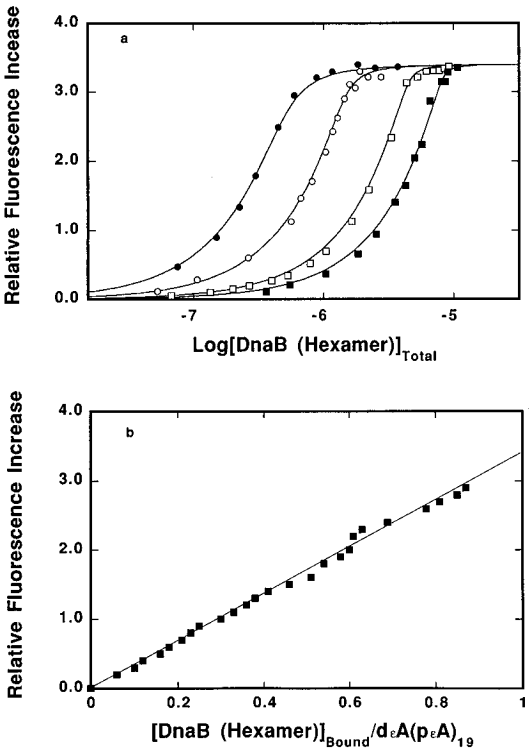

FIGURE 5: a. Fluorescence titrations of dϵA(pϵA)$_{19}$ with the DnaB protein monitored by the increase of the nucleic acid fluorescence in buffer T2 (pH 8.1, 10 °C) containing 100 mM NaCl and 1 mM AMP-PNP, at four different nucleic acid concentrations (Oligomer): (●) 4.9×10^{-7} M; (○) 1.5×10^{-6} M; (□) 4.6×10^{-6} M; (■) 8.4×10^{-6} M. Solid lines are computer fits of the single binding site isotherm, $\Delta F = \Delta F_{max} [K_{20} P_F/(1 + K_{20} P_F)]$, with intrinsic binding constant $K = 3 \times 10^7$ M^{-1} and $\Delta F_{max} = 3.4$. b. The dependence of the relative increase of the dϵA(pϵA)$_{19}$ fluorescence upon the average number of DnaB helicase hexamers bound per oligomer. The absolute value of the average number of DnaB helicase hexamers bound per oligomer has been determined using the thermodynamically rigorous approach described in Materials and Methods.

Table 2: Intrinsic Binding Constant K and Stoichiometry of the DnaB Helicase Complexes with Different 20-mers in Buffer T2 (pH 8.1 10 °C) Containing 293 mM NaCl and 1 mM AMP-PNP

	dϵA(ϵA)$_{19}$	dA(pA)$_{19}$	dT(pT)$_{19}$	dC(pC)$_{19}$
K (M^{-1})	4.5×10^6	3×10^7	3×10^7	9×10^7
stoichiometry	1 ± 0.1	1 ± 0.15	1 ± 0.15	1 ± 0.15

The 1:1 stoichiometry of dϵA(pϵA)$_{19}$ binding to the DnaB hexamer is not affected by an ~17-fold increase of the nucleic acid oligomer concentration (Figure 5a). Therefore, if there are other weaker, functional binding sites, their affinities must be at least ~100-fold lower than the affinity of the strong binding site. The ~17-fold increase of the 20-mer concentration would detect such weak sites by showing an increase in the stoichiometry of the complex. The independence of the DnaB hexamer−20-mer stoichiometry

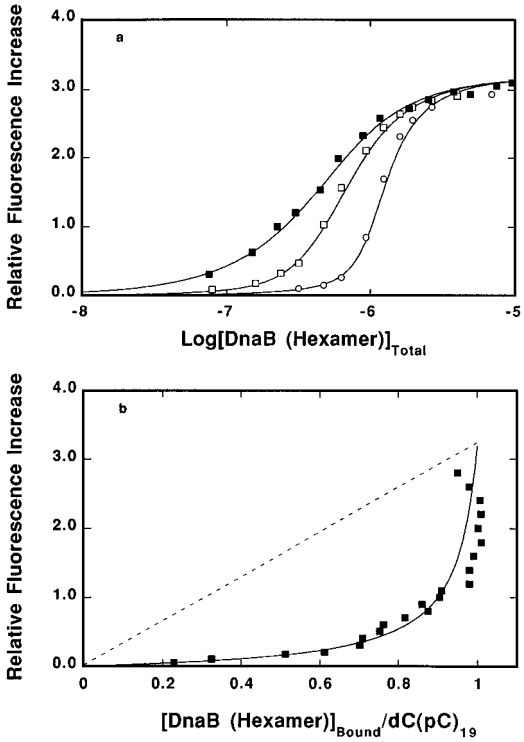

FIGURE 6: a. Fluorescence titrations of dϵA(pϵA)$_{19}$ with the DnaB protein in buffer T2 (pH 8.1, 10 °C) containing 293 mM NaCl and 1 mM AMP-PNP in the presence of two different concentrations of dC(pC)$_{19}$: (□) 2.2×10^{-7} M; (○) 7.3×10^{-7} M (Oligomer) (lattice competition titrations). The titration of dϵA(pϵA)$_{19}$ alone in the same buffer conditions is also included (■). Solid lines are computer fits of the binding isotherms, using equation $\Delta F = \Delta F_{max}[K_{20}P_F/(1 + K_{20}P_F)]$ to describe the binding of the helicase to the reference oligomer, dϵA(pϵA)$_{19}$, with intrinsic binding constant $K_{20} = 4.5 \times 10^6$ M^{-1}, $\Delta F_{max} = 3.2$, and the equation $p = [K_{20}P_F/(1 + K_{20}P_F)]$ [where p is the average number of DnaB hexamer bound per dC(pC)$_{19}$ molecule] to describe the binding to the competing, unmodified 20-mer, using $K_{20} = 9 \times 10^7$ M^{-1} (see Materials and Methods and accompanying paper). b. The dependence of the observed relative fluorescence increase of dϵA(pϵA)$_{19}$ upon the average number of DnaB hexamers bound per dC(pC)$_{19}$ molecule (■). The average number of DnaB hexamers bound per dC(pC)$_{19}$, has been determined, using the MCT method (M. J. Jezewska and W. Bujalowski, accompanying paper). The solid line is the computer simulation of the dependence of the observed fluorescence increase upon the average number of DnaB hexamers bound per dC(pC)$_{19}$ using the independently determined binding constants for both the DnaB−dϵA(pϵA)$_{19}$ and DnaB−dC(pC)$_{19}$ complexes in the same solution conditions (Table 2).

upon nucleic acid concentrations indicates that the hexamer has a single, strong binding site for ssDNA that encompasses 20 nucleotides and that this site is used when the protein binds polymer ss nucleic acid. To further examine this point, we performed studies of the competition between polymer ssDNA and 20-mer for the binding to the DnaB hexamer. Fluorescence titrations of poly(dϵA) with the DnaB helicase in buffer T2 (pH 8.1, 10 °C) containing 100 mM NaCl and 1 mM AMP-PNP at two different dA(pA)$_{19}$ concentrations are shown in Figure 7. In the presence of 20-mer, the binding isotherms are shifted toward higher DnaB protein concentrations. The data show that the oligomer competes very effectively with polymer ssDNA. The solid lines in Figure 7 are computer fits of the DnaB helicase binding to poly(dϵA) (eqs 8 and 11), in the presence of dA(pA)$_{19}$ competing for the same single binding site on the protein hexamer, using $K_{20} = (5 \pm 1) \times 10^7$ M^{-1} for the 20-mer binding to the DnaB protein and the independently determined binding parameters for the DnaB hexamer−poly(dϵA) interactions (Table 1; M. J. Jezewska and W. Bujalowski, accompanying paper). The theoretical lines closely fit the experimental isotherms. It is evident that both the polymer and oligomer ssDNAs compete for the same binding site on the DnaB hexamer.

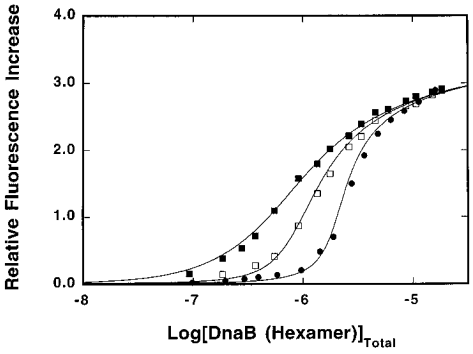

FIGURE 7: Fluorescence titrations of poly(dϵA) with the DnaB protein in buffer T2 (pH 8.1, 10 °C) containing 100 mM NaCl and 1 mM AMP-PNP in the presence of two different concentrations of dA(pA)$_{19}$: (□) 5.5×10^{-7} M; (●) 1.7×10^{-6} M (Oligomer) (lattice competition titrations). The titration of poly(dϵA) alone in the same buffer conditions is also included (■). Solid lines are computer fits of the binding isotherms using the generalized McGhee-von Hippel equation (eqs 8 and 11) to describe the binding of the helicase to poly(dϵA), with intrinsic binding constant $K = 1.3 \times 10^5$ M^{-1}, cooperativity parameter $\omega = 3.5$, and $\Delta F_{max} = 3.5$. The binding of the DnaB protein to dA(pA)$_{19}$ has been described using the equation $p = [K_{20}P_F/(1 + K_{20}P_F)]$ [where p is the average number of DnaB hexamers bound per dA(pA)$_{19}$ molecule] with intrinsic binding constant $K_{20} = 5 \times 10^7$ M^{-1} (see Materials and Methods and accompanying paper).

Intrinsic Affinity and Cooperativity of the Interactions of the DnaB Hexamer With ssDNA. In order to obtain estimations of the intrinsic affinity and cooperativity of the DnaB hexamer binding to single-stranded DNA, the titration curves of poly(dϵA) have been analyzed, using the site-overlap model of McGhee and von Hippel, as defined by generalized eq 8 (Bujalowski et al., 1989). The analysis has been greatly facilitated by an independent determination of the site-size of the DnaB helicase−ssDNA complexes, leaving only two interaction parameters, the intrinsic binding constant, K, and the cooperativity parameter, ω, to be determined.

The solid lines in Figure 2a are computer best fits of the experimental isotherms using eqs 8 and 11. The obtained intrinsic binding constant of the DnaB hexamer binding to poly(dϵA) in buffer T2 (pH 8.1, 10 °C) containing 100 mM NaCl and 1 mM AMP-PNP is $K = (1.3 \pm 0.3) \times 10^5$ M^{-1} and the cooperativity parameter is $\omega = 3.5 \pm 1$. The intrinsic binding constants and cooperativity parameters for different single-stranded homopolymers are included in Table 1. Among the studied polynucleotides, the data indicate a significant DnaB helicase preference for poly(dA). In the standard solution conditions used in this work (50 mM Tris pH 8.1, 10 °C, 100 mM NaCl, 5 mM $MgCl_2$, 1 mM AMP-PNP) binding to poly(dA) is characterized by the intrinsic binding constant, $K = (6 \pm 2) \times 10^6$ M^{-1}, which is comparable to the intrinsic affinities of single-strand binding proteins in corresponding solution conditions (Overman et al., 1988; Kowalczykowski et al., 1981). The lowest intrinsic affinity is observed with poly(dT) [$K = (1 \pm 0.5) \times 10^4$ M^{-1}, Table 1].

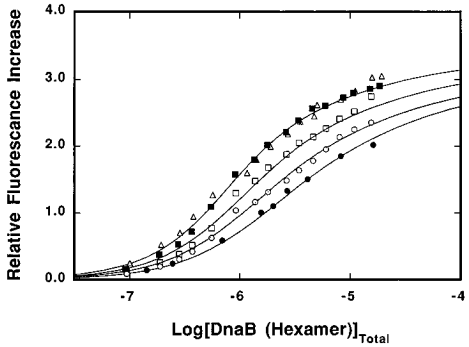

FIGURE 8: Fluorescence titrations of poly(dϵA) with the DnaB protein in buffer T2 (pH 8.1, 10 °C) containing 1 mM AMP-PNP, at different NaCl concentrations: (■) 50 mM; (△) 100 m M; (□) 146 mM; (○) 195 mM; (●) 255 mM. Solid lines are computer fits of the binding isotherms using the generalized McGhee−von Hippel equation (eqs 8 and 11; see text for details).

Binding constants for different DnaB protein−20-mer complexes in buffer T2 (pH 8.1, 10 °C) containing 293 mM NaCl and 1 mM AMP-PNP are included in Table 2. Although both polymer and oligomer nucleic acids bind to the same binding site, the oligomer affinity is much higher when compared to the corresponding polymeric ssDNA. Most probably this reflects preferential interactions of the helicase with the nucleic acid ends (Bujalowski & Jezewska, 1995). The significant contribution of the nonspecific end effect could also be a reason that, contrary to the polymer ssDNA, there is a much less pronounced difference in the affinities among different oligomers (Table 2).

Binding of the DnaB helicase to poly(dϵA), poly(dA), and poly(dC) is characterized by very low cooperativity with $\omega = 3.5 \pm 1$, 6 ± 3, and 5 ± 3, respectively (Table 1, and M. J. Jezewska and W. Bujalowski, accompanying paper). The similar low value of ω for different nucleic acids suggest that the cooperativity is base independent. Determination of the cooperativity in the DnaB helicase binding to polymer ssDNA requires significant saturation of the nucleic acid lattice which is very difficult if the affinity is low. In such cases only an approximate estimation can be made. The estimated upper limit of ω for poly(dT) and poly(dI) is ≤ 10 (Table 1). The independence of ω upon the type of nucleic acid base suggests that it primarily characterizes very weak protein−protein interactions between two bound hexamers. At higher salt concentrations, ω becomes even lower (see next section). Additional information about cooperative interactions between two DnaB hexamers bound to ssDNA can be obtained by studying the protein binding to nucleic acid oligomers. The solid lines in Figure 4a are computer fits of the experimental isotherms of the DnaB protein binding to $d\epsilon A(p\epsilon A)_{39}$, using eq 14, with intrinsic binding constant $K_{40} = 9 \times 10^6$ M^{-1}, cooperativity parameter $\omega = 0.03$, $\Delta F_1 = 2.2$, and $\Delta F_2 = 1.3$. Thus, the binding is characterized by negative cooperativity which is also indicated by the biphasic character of the isotherm (Figure 4a) (Bujalowski & Jezewska, 1995).

Salt Effect on Intrinsic Affinity and Cooperativity of the DnaB Helicase Binding to ssDNA. Fluorescence titrations of poly(dϵA) with the DnaB helicase in buffer T2 (pH 8.1, 10 °C) containing 1 mM AMP-PNP and different NaCl concentrations are shown in Figure 8. As the salt concentration increases, the isotherms shift toward higher total DnaB protein concentrations, indicating a decreasing macroscopic

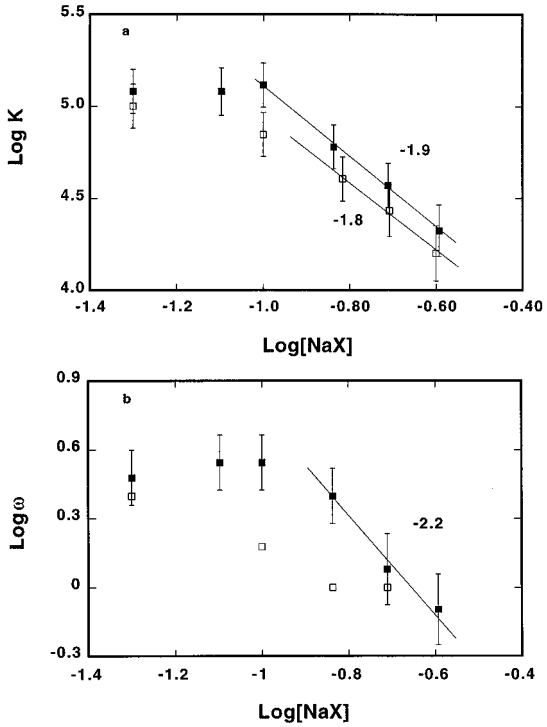

FIGURE 9: a. The dependence of the intrinsic binding constant K for the binding of the DnaB helicase to poly(dϵA) upon NaCl (■) and NaBr (□) concentrations in solution (log−log plots) in buffer T2 (pH 8.1, 10 °C) containing 1 mM AMP-PNP. b. Log−log plot of the dependence of the cooperativity parameter ω for the binding of the DnaB helicase to poly(dϵA) upon NaCl and NaBr concentration in solution in buffer T2 (pH 8.1, 10 °C) containing 1 mM AMP-PNP. The values of the slopes (solid lines) of the linear parts of the plots, in the high salt concentration range, are indicated in the figure.

affinity of the protein−nucleic acid complex at higher salt concentrations. The macroscopic affinity is a complex function of the two processes, the intrinsic binding and cooperative interactions characterized by the intrinsic binding constant, K, and the parameter, ω, respectively. The dependence of the logarithm of the intrinsic binding constant upon the logarithm of [NaCl] (log−log plot) is shown in Figure 9 (closed squares). The plot is clearly nonlinear. Below ∼100 mM NaCl the slope $\partial \log K/\partial \log$ [NaCl] is 0 ± 0.5, although we systematically obtained a slightly higher value of the intrinsic binding constant at 100 mM NaCl when compared to 50 mM NaCl. This suggests an ion uptake accompanying the formation of the complex (Figures 8 and 9). Above 100 mM NaCl the intrinsic affinity dramatically decreases, indicating that the intrinsic binding process is accompanied by a net release of ions. At high salt concentrations, the linear part of the plot is characterized by the $\partial \log K/\partial \log$ [NaCl] $= -1.9 \pm 0.7$, suggesting that a minimum of 2 ions are released upon the complex formation. Essentially, the same salt dependence is observed in the presence of NaBr, although, there is clearly an anion effect, since the intrinsic binding constant is lower by a factor of ∼2 in the presence of NaCl (Figure 9a).

Figure 9b shows the dependence of the cooperativity parameter, ω, on [NaCl] and [NaBr]. As in the case of the intrinsic affinity, the value of ω is slightly affected by increasing the salt concentration up to 100 mM NaCl or NaBr. However, above 100 mM [NaCl], ω decreases significantly and the linear part of the plot at high salt concentrations is characterized by $\partial \log \omega/\partial \log$ [NaCl] =

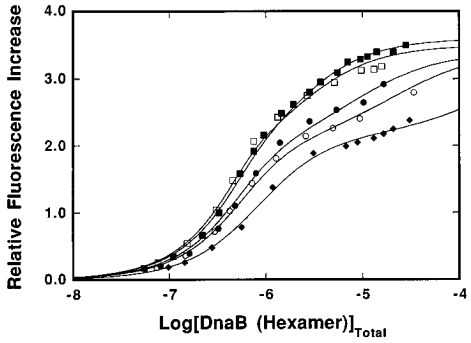

FIGURE 10: Fluorescence titrations of dϵA(pϵA)$_{39}$ with the DnaB protein in buffer T2 (pH 8.1, 10 °C) containing 1 mM AMP-PNP at the following different NaCl concentrations: (■) 50 mM; (□) 100 mM; (●) 147 mM; (○) 195 mM; (♦) 255 mM. Solid lines are computer fits of the binding isotherms, using the statistical thermodynamic model of a large ligand binding to a short homogeneous lattice which can accommodate only two ligand molecules (eqs 13 and 14; see text for details).

-2.2 ± 0.8, indicating the net release of ~2 ions due to the cooperative interactions. Because of the low affinity, the estimation of ω in the presence of NaBr is very difficult at higher salt concentrations. Nevertheless, the log−log plot suggests that a net release of ~2 ions accompanies cooperative interactions.

Fluorescence titrations of dϵA(pϵA)$_{39}$ with the DnaB helicase in buffer T2 (pH 8.1, 10 °C) containing 1 mM AMP-PNP and different NaCl concentrations are shown in Figure 10. Inspection of the isotherms shows that the macroscopic affinity of the second hexamer is affected to a greater extent than the binding of the first DnaB molecule, indicating that the negative cooperativity between the bound hexamers increases with increasing salt concentrations. At high salt concentrations the isotherm separates into two well-defined binding steps. The dependence of the intrinsic binding constant, K_{40}, and cooperativity parameter, ω, on NaCl concentration is shown in Figure 11. Although, the binding constant K_{40} is approximately 2 orders of magnitude larger than the one characterizing the DnaB−poly(dϵA) complex (see above), the dependence of the intrinsic binding process on the salt concentrations is quite similar, with the linear part of the plot at high salt concentrations characterized by the slope $\partial \log K/\partial \log [\mathrm{NaCl}] = -1.9 \pm 0.6$. Similarly, although the value of ω is much lower than the one obtained for the polymer, the salt effect on the negative cooperativity between the two hexamers is characterized by the slope $\partial \log \omega/\partial \log [\mathrm{NaCl}] = -2.3 \pm 0.7$, which is, within experimental accuracy, the same as obtained for poly(dϵA).

Salt Effect on DnaB Helicase−dϵA(pϵA)$_{19}$ Interactions. Fluorescence titration curves of dϵA(pϵA)$_{19}$ with the DnaB protein in buffer T2 (pH 8.1, 10 °C) containing 1 mM AMP-PNP and different NaCl concentrations are shown in Figure 12a. Due to the much higher affinity, we were able to monitor the binding up to ~400 mM NaCl. There is a slight decrease of the maximum of the fluorescence increase at saturation, from 3.4 at 50 mM to 3.2 at 390 mM NaCl. The solid lines in Figure 12a are computer fits to a single-site binding model, with the two fitting parameters, the intrinsic binding constant, K_{20}, and the maximum relative fluorescence increase, ΔF_{max}. Figure 12b shows the dependence of the dϵA(pϵA)$_{19}$ binding constant on NaCl and NaBr concentrations (log−log plot). The linear parts of the plots at high salt concentrations are characterized by the slopes $\partial \log K_{20}/\partial$

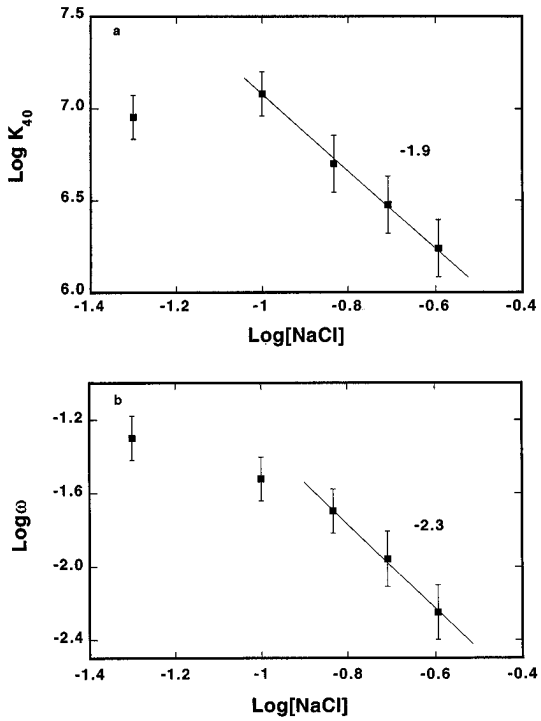

FIGURE 11: a. The dependence of the intrinsic binding constant K_{40} for the binding of the DnaB helicase to dϵA(pϵA)$_{39}$ upon NaCl concentration (■) (log−log plots) in buffer T2 (pH 8.1,10 °C) containing 1 mM AMP-PNP. b. Log−log plot of the dependence of the cooperativity parameter ω for the binding of the DnaB helicase to dϵA(pϵA)$_{39}$ upon NaCl concentration (■) in buffer T2 (pH 8.1, 10 °C) containing 1 mM AMP-PNP. The values of the slopes (solid lines) of the linear parts of the plots, in the high salt concentration range, are indicated in the figure.

$\log [\mathrm{NaCl}] = -3.7 \pm 0.5$ and $\partial \log K_{20}/\partial \log [\mathrm{NaBr}] = -3.4 \pm 0.5$. The values of both slopes indicate that there is a net release of ~3−4 ions upon the complex formation which is higher than the number of ions released in the case of poly(dϵA) and dϵA(pϵA)$_{39}$. It should also be noted that, although the slopes are quite similar, there is an anion effect on the interactions reflected in the intrinsic binding constant, which is lower by a factor of ~2 in the presence of NaBr, when compared with the binding constant in the analogous NaCl concentrations (see Discussion).

Interactions of the DnaB Helicase with Polyribonucleotides. To assess the role of the sugar−phosphate backbone in the DnaB helicase−ss nucleic acid interactions, we performed studies of the DnaB protein binding to homopolyribonucleotides, using the MCT method (Materials and Methods, accompanying paper).

Fluorescence titrations of poly(dϵA) with the DnaB helicase in buffer T2 (pH 8.1, 10 °C) containing 100 mM NaCl and 1 mM AMP-PNP, in the presence of competing poly(A) and poly(U), are shown in Figure 13. The reference titration curve of only poly(dϵA) in the same buffer conditions is also included. For easy comparison, the titrations were performed at the same concentrations of the studied polyribonucleotides [1 mM, (Nucleotide)]. The interactions of the DnaB with polyribonucleotides depends on the type of nucleic acid base; however, this dependence is different than in the case of polydeoxynucleotides. Poly(U) shows the highest affinity followed by poly(A) and poly(C). The intrinsic binding constants are $(4 \pm 2) \times 10^4$ M^{-1}, $(6.5 \pm 2) \times 10^3$ M^{-1}, and ~10^2 M^{-1} for poly(U), poly(A), and poly(C), respectively (see Table 1). These affinities are 2−3

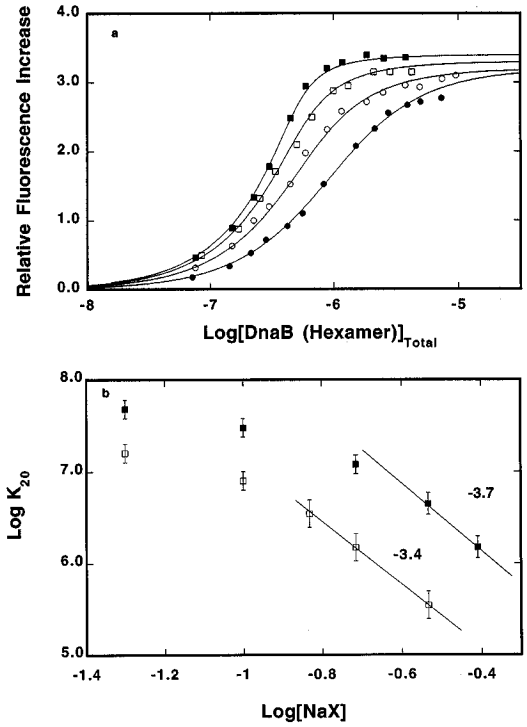

FIGURE 12: a. Fluorescence titrations of dϵA(pϵA)$_{19}$ with the DnaB protein in buffer T2 (pH 8.1, 10 °C) containing 1 mM AMP-PNP at the following different NaCl concentrations: (■) 100 mM; (□) 193 mM; (○) 293 mM; (●) 390 mM. Solid lines are computer fits of the binding isotherms, using equation $\Delta F = \Delta F_{max}\,[K_{20}P_F/(1 + K_{20}P_F)]$ to describe the binding of the helicase to the oligomer, using $\Delta F_{max} = 3.4$ for the titrations at 50 mM and 100 mM NaCl and $\Delta F_{max} = 3.2$ for the titrations at 293 and 390 mM NaCl. b. The dependence of the intrinsic binding constant K_{20} of the DnaB helicase−dϵA(pϵA)$_{19}$ complex upon NaCl (■) and NaBr (□) concentrations (log−log plots) in buffer T2 (pH 8.1, 10 °C) containing 1 mM AMP-PNP. The values of the slopes (solid lines) of the linear parts of the plots in the high salt concentration range are indicated in the figure.

orders of magnitude lower than the affinities for the corresponding polydeoxyribonucleotides (Table 1, see Discussion). Due to the low affinity, only approximate estimations of the cooperativity in the DnaB helicase binding to polyribonucleotides can be obtained, providing $\omega \leq 5$. Figure 13 shows computer fits of the binding of the DnaB helicase to poly(dϵA) in the presence of competing poly(U) and poly(A). The binding of the helicase to poly(dϵA) is described by the generalized McGhee−von Hippel model (eqs 8 and 11), and the binding to poly(U) and poly(A) is described by the Epstein combinatorial theory (M. J. Jezewska and W. Bujalowski, accompanying paper).

Photo-Cross-Linking dT(pT)$_{19}$, dT(pT)$_{55}$, and dT(pT)$_{69}$ to the DnaB Helicase Hexamer. UV irradiation is a widely used method for studying the structure of protein−nucleic acid complexes (Williams & Konigsberg, 1991). Irradiation produces covalent linkage between nucleic acid bases and amino acid residues. The reaction is believed to occur through free-radical mechanisms between photo-excited nucleic acid bases and the amino acid residues which are in very close proximity and to produce "zero-length" cross-linking with minimal perturbation to the studied protein−nucleic acid complex. Among the nucleic acid bases, thymine is by far the most reactive in the photo-cross-linking reactions. Previously, we have shown that the oligomer dT(pT)$_{19}$, which exactly spans the site-size of the DnaB

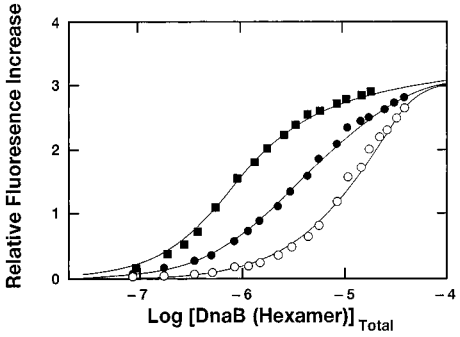

FIGURE 13: Fluorescence titrations of poly(dϵA) [2×10^{-5} M (Nucleotide)] with the DnaB protein in buffer T2 (pH 8.1, 10 °C) containing 100 mM NaCl and 1 mM AMP-PNP, in the presence of poly(U) (○) and poly(A) (●) (lattice competition titrations). The titration of poly(dϵA) alone in the same buffer conditions is also included (■). The concentrations of each polyribonucleotide is 1 mM (Nucleotide). Solid lines are computer fits of the binding isotherms using the generalized McGhee−von Hippel equation (eqs 8 and 11) to describe the binding of the helicase to poly(dϵA), with intrinsic binding constant $K = 1.3 \times 10^5$ M^{-1}, cooperativity parameter $\omega = 3.5$, and $\Delta F_{max} = 3.5$. The binding of the DnaB protein to polyribonucleotides has been described by the Epstein combinatorial theory (M. J. Jezewska and W. Bujalowski, accompanying paper) using intrinsic binding constants $K = 6.5 \times 10^3$ and 4×10^4 M^{-1}, $n = 20$, and cooperativity parameter $\omega = 3$ for poly(A) and poly(U), respectively.

helicase−ssDNA complex, efficiently cross-links with only a single subunit of the hexamer (Bujalowski & Jezewska, 1995). We performed photo-cross-linking experiments of the DnaB−dT(pT)$_{19}$ complex parallel to our thermodynamic binding studies at different solution conditions. Figure 14a shows the autoradiogram of the SDS polyacrylamide gel of the DnaB−(dT)$_{20}$ complex after irradiation in buffer T2 (pH 8.1, 10 °C) containing 100 mM NaCl and 1 mM AMP-PNP at different nucleic acid concentrations. Only a single radioactive band appears on the gel, at the molecular weight of ∼58 000, corresponding to the DnaB monomer−(dT)$_{20}$ complex. The same result is obtained at different salt concentrations (data not shown) indicating that, independently of the solution conditions, a single subunit efficiently photo-cross-links with 20-mer. Due to the increased irradiation time (30 min) a slight, additional protein band appears at the molecular weight of ∼150 000 on Coomassie Brilliant Blue stained gels, indicating limited photo-cross-linking between DnaB subunits (Figure 14b,d). Because no corresponding radioactive bands are visible on autoradiograms of the same gels (Figure 14a,c) the intersubunit photo-cross-linking must occur between several protomers of the hexamer not involved in the ss nucleic acid binding.

The photo-cross-linking results of the DnaB hexamer−(dT)$_{20}$ complex indicate that only a limited set of subunits of the hexamer, and most probably only one, is engaged in interactions with ssDNA (Figure 14a). To further address this point, we have performed photo-cross-linking experiments with oligomers dT(pT)$_{55}$ and dT(pT)$_{69}$, which are significantly longer than the determined site-size of the helicase−ssDNA complex. Figure 14c shows the autoradiogram of the SDS polyacrylamide gel of the DnaB−[5′-^{32}P]-(dT)$_{20}$, DnaB−[5′-^{32}P]-(dT)$_{56}$, and DnaB−[5′-^{32}P]-(dT)$_{70}$ complexes. The concentration of each nucleic acid is kept constant, and the concentration of the helicase varies. First, in all cases, only a single principal radioactive band is visible. Second, each radioactive band is shifted toward a higher molecular weight, with the increased molecular weight of

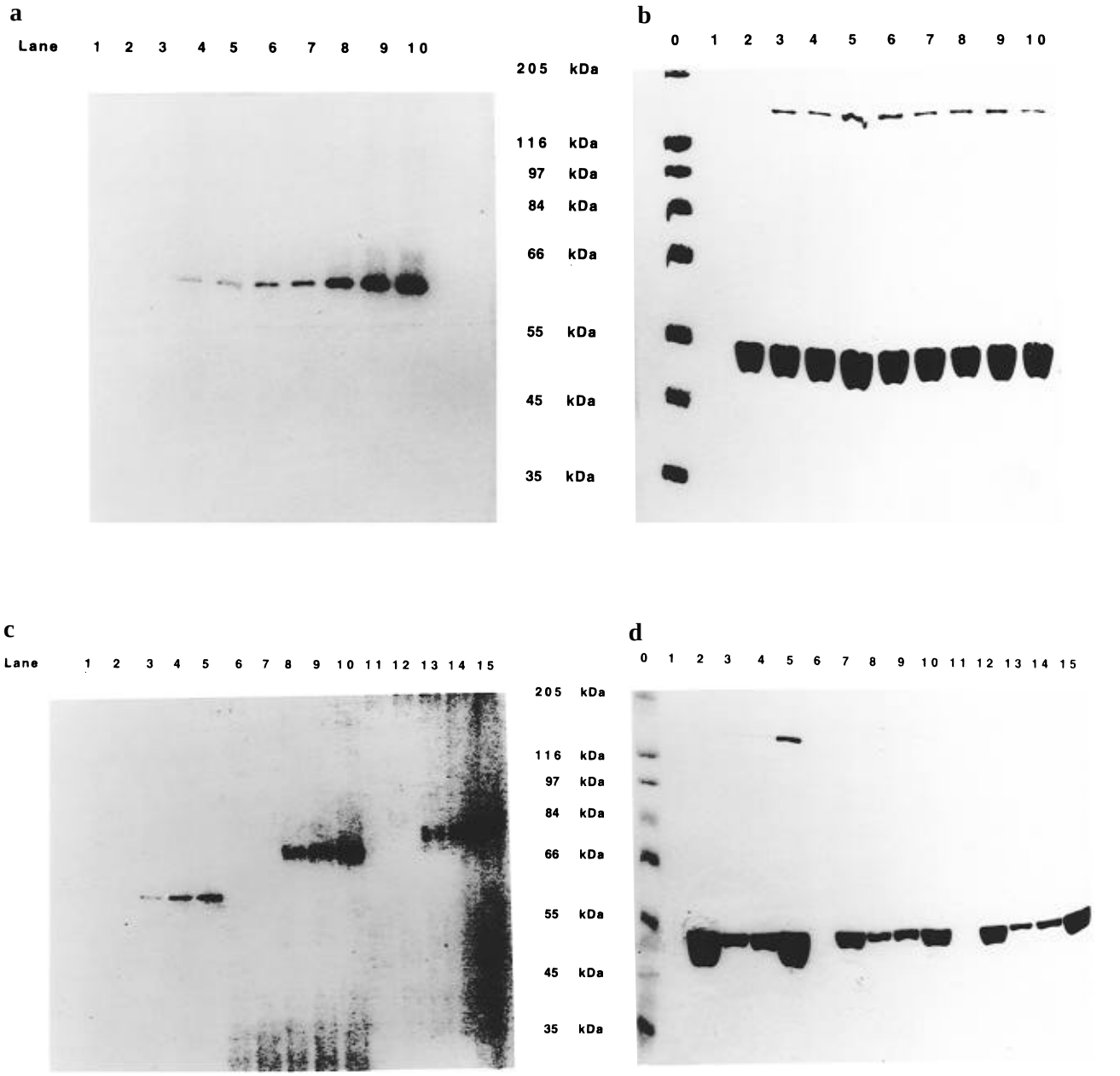

FIGURE 14: a. Autoradiogram of the SDS polyacrylamide gel electrophoresis of the DnaB protein−[5′-^{32}P]-$(dT)_{20}$ complexes, after UV-mediated cross-linking of the nucleic acid to the helicase, in buffer T2 containing 100 mM NaCl and 1 mM AMP-PNP. Lane 1 shows [5′-^{32}P]-$(dT)_{20}$ alone, and lane 2 shows the control sample which is a nonirradiated mixture of [5′-^{32}P]-$(dT)_{20}$ = 1×10^{-6} M (Oligomer) with [DnaB] = 1×10^{-6} M (Hexamer). In Lanes 3−10, the concentration of the protein was kept constant ([DnaB] = 1×10^{-6} M) and the concentration of the [5′-^{32}P]-$(dT)_{20}$ was varied: lane 3, 1×10^{-7} M (Oligomer); lane 4, 2×10^{-7} M; lane 5, 5×10^{-7} M; lane 6, 1×10^{-6} M; lane 7, 2×10^{-6} M; lane 8, 5×10^{-6} M; lane 9, 8×10^{-6} M; lane 10, 1.3×10^{-5} M. b. The same polyacrylamide gel as shown in 1a, aligned exactly with an autoradiogram and stained with Coomassie Brilliant Blue. Lane 0 contains molecular weight markers. c. Autoradiogram of the SDS polyacrylamide gel electrophoresis of DnaB protein−[5′-^{32}P]-$(dT)_{20}$, DnaB protein−[5′-^{32}P]-$(dT)_{56}$, DnaB protein−[5′-^{32}P]-$(dT)_{70}$ complexes, after UV-mediated cross-linking of the nucleic acid to the helicase in buffer T2 containing 100 mM NaCl and 1 mM AMP-PNP. Lanes 1, 6, and 11 show [5′-^{32}P]-$(dT)_{20}$, [5′-^{32}P]-$(dT)_{56}$, and [5′-^{32}P]-$(dT)_{70}$, alone; lanes 2, 7, and 12 show the control samples which are the nonirradiated mixtures of [5′-^{32}P]-$(dT)_{20}$ = 3×10^{-6} M (Oligomer) with [DnaB] = 3×10^{-6} M (Hexamer), [5′-^{32}P]-$(dT)_{56}$ = 1×10^{-6} M (Oligomer) with [DnaB] = 1×10^{-6} M (Hexamer), and [5′-^{32}P]-$(dT)_{70}$ = 1×10^{-6} M (Oligomer) with [DnaB] = 1×10^{-6} M (Hexamer). In lanes 3−5, the concentration of the [5′-^{32}P]-$(dT)_{20}$ was kept constant (1×10^{-6} M) and the concentration of the protein was varied: lane 3, 3.8×10^{-7} M; lane 4, 6×10^{-7} M; lane 5, 3×10^{-6} M. In lanes 7−10, the concentration of the [5′-^{32}P]-$(dT)_{56}$ was kept constant (1×10^{-6} M) and the concentration of the protein was varied: lane 8, 1.25×10^{-7} M; lane 9, 2×10^{-7} M; lane 10, 1×10^{-6} M. In lanes 13−15 the concentration of the [5′-^{32}P]-$(dT)_{70}$ was kept constant (1×10^{-6} M) and the concentration of the protein was varied: lane 13, 1.25×10^{-7} M; lane 14, 2×10^{-7} M; lane 15, 1×10^{-6} M. d. The same polyacrylamide gel as shown in c, aligned exactly with the autoradiogram and stained with Coomassie Brilliant Blue. Lane 0 contains molecular weight markers.

the nucleic acid in the complex. The bands are located at apparent molecular weights ~58 000, ~70 000, and ~75 000, corresponding very closely with the expected molecular weight of the DnaB monomer−$(dT)_{20}$, DnaB monomer−$(dT)_{56}$, and DnaB monomer−$(dT)_{70}$ complexes, respectively. It is evident that even with the ssDNA oligomers, much larger than the site-size of the helicase−nucleic acid complex, only a single subunit of the hexamer predominantly cross-links with the ssDNA.

Sedimentation Velocity Studies of the DnaB Helicase−ssDNA Complexes. Analytical ultracentrifuge experiments can provide independent information about the stoichiometry

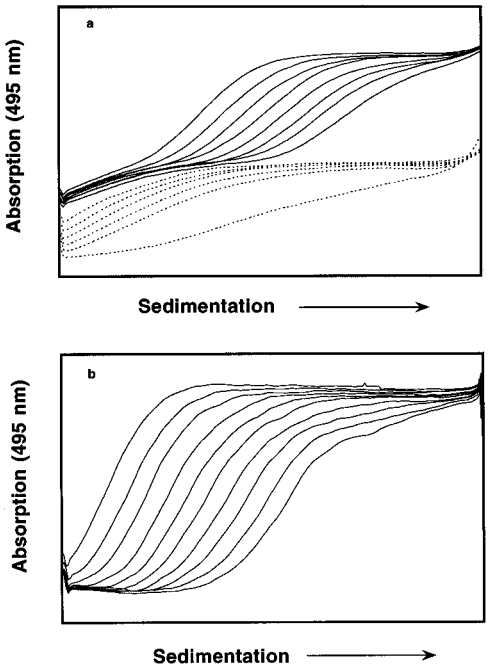

FIGURE 15: a. Absorption profiles at 495 nm of the sedimentation velocity runs of 5′-fluorescein-$(dT)_{20}$−DnaB protein complex in buffer T2 (pH 8.1, 20 °C) containing 100 mM NaCl and 1 mM AMP-PNP, at 1.9:1 molar excess of the nucleic acid over the enzyme (8 min time interval). The concentration of the DnaB hexamer is 3.1×10^{-6} M, and the concentration of the 5′-fluorescein-$(dT)_{20}$ is 5.84×10^{-6} M (Oligomer). Solid lines are initial scans of the samples performed at 30 000 rpm. Dashed lines are scans of the sample performed at 60 000 rpm, after the fast moving boundary reached the bottom of the cell. The initial part of the last scan indicates the location of the base line. b. Absorption profiles at 495 nm of the sedimentation velocity run of 5′-fluorescein-$(dT)_{20}$−DnaB protein complex, in buffer T2 (pH 8.1, 20 °C) containing 100 mM NaCl and 1 mM AMP-PNP, at 3:1 molar excess of the DnaB protein over the nucleic acid. The concentration of the DnaB hexamer is 8.88×10^{-6} M and the concentration of the 5′-fluorescein-$(dT)_{20}$ is 2.92×10^{-6} M (Oligomer); 8 min time interval; 30 000 rpm.

and structure of the DnaB−ssDNA complex (Tanford, 1961). However, the analysis of the sedimentation absorption profiles of the protein−nucleic acid mixture is difficult because both macromolecules absorb in the same UV region. In order to be able to monitor only one component, we performed the sedimentation experiments with the $dT(pT)_{19}$ oligomer labeled specifically at its 5′-end with fluorescein [5′-fluorescein-$(dT)_{20}$]. Binding affinity (K_{20}) of this oligomer to the DnaB helicase is essentially the same as the affinity of the parental $dT(pT)_{19}$ (Table 2, M. J. Jezewska and W. Bujalowski, manuscript in preparation).

The sedimentation velocity profiles (monitored at 495 nm) of the DnaB helicase−5′-fluorescein-$(dT)_{20}$ complex at 1.9:1 molar ratio of the nucleic acid over the helicase hexamer in buffer T2 (pH 8.1, 20 °C) containing 100 mM NaCl and 1 mM AMP-PNP are shown in Figure 15a. The concentrations of the enzyme and the nucleic acid were selected to provide stoichiometric binding (Table 2). The sedimentation run has been initially performed at 30 000 rpm (solid lines). There are clearly two independently moving boundaries. The slow moving boundary has a sedimentation coefficient of $s_{20,w} = 1.4 \pm 0.2$ which is the value of the free 5′-fluorescein-$(dT)_{20}$. The fast moving boundary contains 5′-fluorescein-$(dT)_{20}$ in the complex with the DnaB helicase and has a sedimentation coefficient of $s_{20,w} = 12.2 \pm 0.3$. Independent equilibrium sedimentation studies show that the DnaB hexamer fully preserves its hexameric structure in the complex with the ssDNA 20-mer (data not shown). After the fast moving boundary reached the cell bottom, the sedimentation run was continued at 60 000 rpm (dashed lines). Notice, during the sedimentation process the boundary of the complex migrates in the region of constant free 20-mer concentration $\gg 1/K_{20}$ (Table 2), thus assuring that the enzyme is always saturated with the nucleic acid. At 495 nm one monitors exclusively the concentration of the 20-mer. Comparison of the contributions of the slow and fast moving boundaries to the total absorption of the sample shows that 55% of the total nucleic acid concentration migrated in the fast moving boundary (Figure 15a). From the known total concentration of the DnaB helicase in the sample, the stoichiometry of the complex is calculated to be 0.95 ± 0.05 which is identical to the stoichiometry of the DnaB−20-mer complex independently determined by the rigorous fluorescence titration technique (see above). These results also directly establish that the DnaB hexamer is the species which binds ssDNA.

Sedimentation velocity profiles of the mixture of the DnaB helicase and 5′-fluorescein-$(dT)_{20}$, in buffer T2 (pH 8.1, 20 °C) containing 100 mM NaCl and 1 mM AMP-PNP, in the 3:1 molar excess of the enzyme over the nucleic acid are shown in Figure 15b. Because the [DnaB] $\gg 1/K_{20}$, all nucleic acid should be complexed with the helicase. As a result, only a single boundary of the complex is observed throughout the entire sedimentation process, with a sedimentation coefficient of $s_{20,w} = 12.3 \pm 0.2$. This value, within experimental accuracy, is the same as the one obtained in experiments where the molar excess of the nucleic acid was applied (Figure 15a).

The sedimentation coefficient of the ternary complex, DnaB−(AMP-PNP)−5′-fluorescein-$(dT)_{20}$ is significantly higher (∼17%) than the sedimentation coefficient of the free enzyme ($s_{20,w} = 10.5 \pm 0.3$) in the same solution conditions (Bujalowski et al., 1994). This is in spite of the fact that the bound nucleic acid and the bound AMP-PNP constitute only ∼3% of the molecular weight of the protein hexamer. This large change of hydrodynamic properties of the helicase associated with the ternary complex formation indicates that, in the complex, the enzyme undergoes dramatic conformational changes which encompass all six subunits of the hexamer.

DISCUSSION

Stoichiometry of the DnaB Helicase−ssDNA Complex Is Independent of the Type of Nucleic Acid Base and Salt Concentration. The physiological role of the DnaB helicase is strictly related to the ability of the enzyme to interact with ss and dsDNA under ATP control. Yet, little is known about the quantitative molecular mechanism of the hexameric replicative helicase−nucleic acid interactions. In this communication, we provide extensive quantitative studies of the stoichiometry, free energy of binding, cooperativity, structure, and the effect of solution conditions (salt) on the DnaB hexamer interactions with ss nucleic acids.

Quantitative studies of the interactions of the DnaB protein with ssDNA are greatly facilitated by the finding that binding of the protein to the fluorescent etheno analog of poly(dA), poly(dϵA), is accompanied by a strong increase of nucleic acid fluorescence (Figure 1; Bujalowski & Jezewska, 1995).

At the excitation wavelength applied (λ_{ex} = 325 nm), only ethenoadenosine is excited. Thus the observed increase results from an increase of the quantum yield of the nucleic acid in the complex with the helicase. The fluorescence of ϵA is dramatically quenched (8−10-fold) in etheno oligomers and poly(ϵA) as compared to free ϵAMP (Tolman et al., 1974; Baker et al., 1978; Kubota et al., 1983). Stacking interactions between neighboring ϵA bases is similar to stacking interactions in unmodified adenosine polymers (Baker et al., 1978). A dynamic model in which the motion of ϵA leads to quenching via intramolecular collision has been proposed as a predominant mechanism of the observed strong quenching (Baker et al., 1978). Increased viscosity of the solvent leads to a decreased base mobility and partially eliminates the fluorescence quenching.

The observed strong increase of the etheno derivative oligomers and poly(dϵA) upon binding to the DnaB helicase may result from significantly restricted mobility of the nucleic acid bases in the complex with the enzyme. Indeed, our preliminary data show a strong increase of the fluorescence anisotropy of dϵA(pϵA)$_{19}$ in the complex with the DnaB protein (M. J. Jezewska and W. Bujalowski, accompanying paper). It is possible that a similar, strong increase of the fluorescence of the etheno derivatives of DNA, in the complex with the DnaB helicase, will also occur upon the binding of other helicases, hence allowing the determination of equilibrium interaction parameters in solution with both polymer and oligomer nucleic acids.

Quantitative analysis of the binding of the DnaB hexamer to a fluorescent etheno derivative ssDNA has been performed, using the approach which allowed us to determine the thermodynamically rigorous binding parameters without assuming the relationship between the observed signal (fluorescence in this case) and the degree of lattice saturation (Bujalowski & Jezewska, 1995). The analogous, rigorous MCT method described in the accompanying paper, has been applied to determine the binding parameters for nonfluorescent, unmodified ssDNA. Both direct binding studies of the DnaB helicase interactions with etheno derivatives of ssDNA and competition experiments with unmodified, nonfluorescent polymeric and oligomeric ss nucleic acids, in different solution conditions, show that the DnaB helicase binds ssDNA with the stoichiometry of 20 ± 3 nucleotides per hexamer. Thus, the stoichiometry of the complex is independent of the type of nucleic acid base, as well as salt concentrations and type of salt. These results are particularly important in light of the suggestion that the DnaB hexamer forms a specific complex structure with some ss polynucleotides, especially poly(dT) (Arai & Kornberg, 1981b). Our thermodynamic and sedimentation velocity studies of the DnaB−dT(pT)$_{19}$ interactions show that the oligomer competes for the same binding site with dϵA(pϵA)$_{19}$ and that the oligomer binds the helicase with a 1:1 stoichiometry, which is the same as the stoichiometry of the complex of the helicase with any other 20-mer (Table 2, Figure 15a). Using the MCT method, we performed additional binding studies of the DnaB helicase to dT(pT)$_{39}$ and dT(pT)$_{69}$ (data not shown). Two and three DnaB hexamers bind to the 40-mer and the 70-mer at saturation, in excellent agreement with the stoichiometries determined with other ss polynucleotides in this work.

DnaB Hexamer Has a Single, Strong ssDNA Binding Site. Binding experiments with dϵA(pϵA)$_{19}$ show that even an ~17-fold increase of the oligomer concentration does not change the 1:1 stoichiometry of the complex (Figure 5a), indicating that the hexamer has a single, strong binding site for ssDNA. Although linear dependence of the poly(dϵA) fluorescence upon $\sum\nu_i$ strongly indicates that a single type of complex is formed between DnaB and poly(dϵA), it is still possible that some weak sites could participate in the binding of the DnaB hexamer to polymer ssDNA. This possibility can be tested by competition binding experiments between the polymer ssDNA and the 20-residues long oligomer and photo-cross-linking studies with ssDNA oligomers of different lengths (see below). Fluorescence titrations of poly(dϵA) with the DnaB helicase in the presence of dA(pA)$_{19}$ show that the oligomer competes very efficiently with poly(dϵA). Also computer simulations of the competition between poly(dϵA) and 20-mer for the same binding site using independently determined binding parameters for the polymer and oligomer fit the experimental isotherms remarkably well. Thus, the results obtained indicate that both nucleic acids compete for the same binding site or, in other words, that the same binding site that encompasses 20 nucleotides is used when the DnaB hexamer binds to polymer or oligomer ssDNA.

In their pioneering studies of DnaB protein−ssDNA interactions, Arai and Kornberg (1981b) suggested, on the basis of the Scatchard plot of the binding of (dT)$_{14}$ to the DnaB protein which was obtained using filter binding assay experiments, that there must be at least four equivalent binding sites for ssDNA on the DnaB hexamer. They also suggested, on the basis of nuclease digestion−protection experiments, that the site-size of the complex probably encompasses a stretch of ~80 nucleotides. However, it should be pointed out that the resolution in their nuclease digestion−protection experiments was low, with ssDNA fragments ranging from 15 to 80 nucleotides in length. Moreover, the filter binding assay is a nonequilibrium technique which may lead to significant perturbation of the studied equilibrium making a quantitative evaluation difficult. It should also be remembered that these early studies were performed when the exact concentration of the DnaB protein could not be determined. Using thermodynamically rigorous equilibrium fluorescence titration methods we have established that the site-size of the DnaB helicase−ssDNA complex is only 20 ± 3 nucleotides and that there is a single, strong binding site for ssDNA on the hexamer.

Only a Limited Set of Subunits of the DnaB Hexamer Is Predominantly Engaged in Interactions with ssDNA. Our hydrodynamic studies indicate that in the DnaB hexamer the protomers form a cyclic structure with each protomer having contact with only two other subunits (Bujalowski et al., 1994). Recent electron microscopy studies also show the cyclic structure of the DnaB hexamer, with each subunit in contact with only two of its neighbors (San Martin et al., 1995). Estimation of the distance of 30−40 Å between the centers of mass of neighboring subunits suggests that the ss nucleic acid of 20 nucleotides in length is just long enough to contact only one or two subunits (Bujalowski & Jezewska, 1995). The additional insight in the number of subunits involved in the ssDNA binding can be obtained by studying the photo-cross-linking of the ssDNA oligomers of different lengths to the DnaB hexamer. We have previously shown that at lower salt concentrations the oligomer dT(pT)$_{19}$ efficiently cross-links with the DnaB protein (Bujalowski &

Jezewska, 1995). The results shown in Figure 14a indicate that, independently of the increasing concentration of dT-$(pT)_{19}$, only a single radioactive band appears on the SDS polyacrylamide gel around the molecular weight of ∼58 000, corresponding with the expected molecular weight of the dT-$(pT)_{19}$−DnaB monomer complex. These results do not change upon increasing the [NaCl] up to 390 mM, the highest salt concentration studied (data not shown). It is still possible that, in the case of a longer ssDNA, another subunit may become involved in the nucleic acid binding. We performed photo-cross-linking studies of the DnaB protein complexes with oligomers $dT(pT)_{55}$ and $dT(pT)_{69}$. In both cases, only a single, major radioactive band, located around the molecular weight and corresponding very closely with the expected molecular weight of the DnaB monomer−ss oligomer complex, is observed (Figure 14c). Clearly, even in the presence of ssDNA significantly longer than the site-size of the complex, only a single subunit of the hexamer is primarily engaged in interactions with the ss nucleic acid.

Intrinsic Affinity of the DnaB Protein−ss Nucleic Acid Interactions Depends upon the Type of Nucleic Acid Base and Salt Concentration. There is a significant difference in the intrinsic affinity of the DnaB helicase for ssDNA, differing by the type of base. In interactions with the polymer ssDNA, the enzyme shows the highest affinity for poly(dA) and the lowest affinity for poly(dT) which would suggest an important contribution of the base in ssDNA binding (Table 1). On the other hand, the affinities of the DnaB helicase toward the polyribonucleotides, including poly(A), are dramatically lower when compared with the polydeoxyribonucleotides, suggesting that the sugar−phosphate backbone provides a significant contribution to the intrinsic free energy of binding. However, both contributions do not seem to be simply additive, as indicated by a much lower affinity of poly(A), when compared to poly(U) (Table 1). The obtained data suggest that the affinity of polydeoxyribonucleotides results from the complex interplay between two elements, the deoxyribose of the sugar−phosphate backbone and the base.

It has been suggested that, partly due to its very low affinity toward ssDNA, the DnaB helicase has to be "delivered" at the oriC site in the complex with the DnaC protein (Whale et al., 1989). The role of the DnaC protein would simply be to facilitate the loading of the DnaB helicase on ssDNA. However, the results obtained in this work indicate that the helicase possesses a relatively high affinity toward ssDNA, particularly for poly(dA), and suggest that the highly specific role of the DnaB−DnaC complex, in the initiation of the DNA replication, results more from specific protein−protein interactions required at the replication origin (oriC) than from the simple process of facilitating the binding of the enzyme to the ssDNA lattice (Allen & Kornberg, 1991).

The effect of salt on the interactions of the DnaB helicase with polymer ssDNA indicates that both the intrinsic affinity and cooperative interactions are accompanied by a net release of ∼2 ions (Figure 9a,b). Quantitatively, the same salt effect is observed in the interaction of the DnaB helicase with dϵA-$(p\epsilon A)_{39}$, although the intrinsic affinity is higher and there is negative cooperativity in the binding (Figure 11). Because the thermodynamic degree of cation binding on nucleic acids should not significantly change in the studied salt concentration ranges, the nonlinear behavior of the log−log plot suggests that some of the released ions originate from the protein (Record et al., 1976). This conclusion is further supported by the clear difference between Cl^- and Br^- in affecting the intrinsic affinity and cooperative interactions. However, it should be mentioned that because of the presence of multiple components in solution, the studied system is extremely complex. A strong decrease of the intrinsic binding constant of the DnaB protein−nucleic acid complex, independently of the length of nucleic acid, occurs around 100 mM NaCl and NaBr and suggests that the ions are released from the binding sites which are characterized by the affinity constant of at least 20 M^{-1}. The higher number of released ions (∼3−4) in the binding of 20-mer to the DnaB protein is rather surprising (Figure 12). Due to its oligomeric nature, the thermodynamic degree of cation binding to this nucleic acid should be lower, when compared to the polymer ssDNA and the 40-mer (Olmsted et al., 1989). On the other hand, if the released ions mainly originate from the protein, the larger number of released ions may result from the detected differences between the DnaB−polymer ssDNA and the DnaB−20-mer complexes, as expressed by a much higher affinity (∼2 orders of magnitude) of the 20-mer for the ssDNA binding on the enzyme, when compared to the longer nucleic acids.

Binding of the DnaB helicase to ssDNA is characterized by a very low value of the cooperativity parameter, ω, which becomes even lower at high salt concentrations (Table 1, Figures 9 and 11). The low value of ω and its independence upon the type of nucleic acid base suggests that it characterizes weak interactions between bound DnaB hexamers. Comparison with other replicative helicases is difficult because, to our knowledge, no quantitative data on the interactions of a replicative helicase−polymer ssDNA are yet available for other enzymes. However, the fact that the DnaB hexamer is not able to form long protein clusters, when bound to ssDNA, may reflect a general aspect of the functioning of a replicative helicase (Bujalowski & Jezewska, 1995). The initiation of the replication from a specific site (oriC) and the processive unwinding of the dsDNA at the junction between ss and dsDNA in the replication fork does not require clusters of helicase molecules. Very weak protein−protein interactions, independent of the type of the nucleic acid base, may be a simple evolutionary adaptation of the replicative helicase which allows the enzyme to perform functions requiring a single protein molecule.

Long-Range Allosteric Interactions in the DnaB Helicase Hexamer. The DnaB hexamer is built of six chemically identical protomers. It is most probable that all six protomers are initially capable of binding ATP and ssDNA (Bujalowski & Klonowska, 1993). The presence of a single, strong ssDNA binding site, predominately located on a single subunit of the hexamer saturated with AMP-PNP indicates the existence of very complex, long-range allosteric interactions among ATP and ssDNA binding sites which encompass *all six subunits* of the hexamer. These long-range interactions, on the level of quaternary structure of the hexameric enzyme leading to the selection of a limited set of subunits as a binding site for ssDNA, would require significant conformational changes of the hexamer, far beyond the nearest neighboring protomers.

The sedimentation velocity studies reported in this work provide the direct evidence of such long-range conformational changes within the protein hexamer, as a result of the

formation of the ternary complex, DnaB−(AMP-PNP)−ssDNA. The sedimentation coefficient of the ternary complex, $s_{20,w} = 12.3 \pm 0.2$, is ∼17% larger than the sedimentation coefficient of the free enzyme ($s_{20,w} = 10.5 \pm 0.3$; Bujalowski et al., 1994). Because the bound nucleic acid and the nucleotide [5′-fluorescein-$(dT)_{20}$ and AMP-PNP] constitute only ∼3% of the DnaB hexamer molecular weight, this large change in the sedimentation coefficient of the hexamer in the complex does not simply result from the increased molecular weight of the complex, or a trivial effect of the lower partial specific volumes of the bound nucleic acid and nucleotide molecules. In fact, the sedimentation velocity studies, in which a single 10-mer molecule is bound per DnaB hexamer, provide the same increase of the sedimentation coefficient of the complex as 20-mer, although they differ by as much as 10 nucleotide residues (M. J. Jezewska and W. Bujalowski, manuscript in preparation). Thus, the dramatic change in the hydrodynamic properties of the enzyme in the ternary complex results from long-range allosteric interactions, including the entire DnaB hexamer. In this context, it should be pointed out that our thermodynamic studies of nucleotide binding to the DnaB hexamer have provided the first indication of cooperative interactions on the level of the quaternary structure of the hexameric enzyme (Bujalowski & Klonowska 1993, 1994a,b). However, these interactions were proposed to be limited to only two adjacent protomers, leading to a biphase binding isotherm.

The results obtained in this study and our previous work (Bujalowski & Jezewska, 1995) have a profound significance for formulating a model of the hexameric replicative helicase translocation on nucleic acids and the mechanism of dsDNA unwinding. The very low site-size of the large DnaB hexamer−ssDNA complex and the presence of only a single, strong ssDNA binding site, most probably located on a single subunit of the hexamer, preclude any extensive wrapping of the nucleic acid around all six subunits of the hexamer and the formation of a nucleosome-like structure (Bujalowski & Jezewska, 1995). Both the hydrodynamic and EM data indicate the existence of a cross channel in the cyclic structure of the DnaB hexamer with a diameter of approximately 30−40 Å (Bujalowski et al., 1994; San Martin et al., 1995). Although speculative at this time, the results of the thermodynamic measurements of the stoichiometry of the complex, the photo-cross-linking experiments, the hydrodynamic and EM data suggest the interesting possibility that the DnaB helicase interactions with ssDNA may belong to the same type of interactions, previously proposed for the sliding clamps of *E. coli* DNA polymerase III holoenzyme, *E. coli* RuvB protein, and bacteriophage T7 helicase/primase protein, in which the ssDNA molecule passes through the crossing channel of the hexamer (Kong et al., 1992; Stasiak et al., 1993; Egelman et al., 1995; San Martin et al., 1995). In such interactions, a much shorter fragment of the ssDNA would be required for the binding of the helicase, compared to the nucleosome type of the complex. Also, contrary to the nucleosome-like complex, in which all subunits are involved in the binding, the cross channel binding model is compatible with only a limited set of subunits, possibly only one, predominately involved in interactions with nucleic acid, when the helicase is bound to ssDNA (Bujalowski & Jezewska, 1995).

In the mobile replication promoter function, the DnaB protein, complexed with ssDNA, provides a recognition complex for the primase (Arai & Kornberg, 1981b). A unique secondary structure of the ssDNA, formed in the complex with the DnaB protein as a result of wrapping the nucleic acid around the protein hexamer, was postulated to be the specific recognition element for primase. Although some limited "wrapping" of ssDNA in the complex with the DnaB hexamer cannot be completely ruled out, results obtained in this work on the stoichiometry of the DnaB−ssDNA complex indicate that this is not the case. It is rather unlikely that a short stretch of 20 nucleotides, engaged in interactions predominantly with one subunit of the hexamer, would form a highly specific secondary structure when bound in the ssDNA binding site of the DnaB helicase. The sedimentation data indicate that the DnaB helicase undergoes specific global conformational changes in the ternary complex with AMP-PNP and ssDNA. Most probably these conformational changes are specifically recognized by the primase through direct protein−protein interactions. Direct physical interactions between the primase and the DnaB helicase have recently been reported (Tougu et al., 1994). The results described in this work provide direct evidence of dramatic conformational changes of the entire DnaB hexamer, as a result of the long-range allosteric interactions within the ternary complex.

ACKNOWLEDGMENT

We thank Dr. J. C. Lee for the use of the model E analytical centrifuge, Dr. E. W. Czerwinski for his careful reading and helpful comments on the manuscript, and Mrs. Gloria Drennan Davis for her help in preparing the manuscript.

REFERENCES

Allen, G. C., & Kornberg, A. (1991) *J. Biol. Chem. 266*, 22096−22101.
Arai, K., & Kornberg, A. (1981a) *J. Biol. Chem. 256*, 5253−5259.
Arai, K., & Kornberg, A. (1981b) *J. Biol. Chem. 256*, 5260−5266.
Baker, B. M., Vanderkooi, J., & Kallenbach, N. R. (1978) *Biopolymers*, *17*, 1361−1372.
Baker, T. A., Funnell, B. E., & Kornberg, A. (1987) *J. Biol. Chem. 262*, 6877−6885.
Bear, D. G., Hicks, P. S., Escudero, K. W., Andrews, C. L., McSwiggen, J. A., & von Hippel, P. H. (1988b) *J. Mol. Biol. 199*, 623−635.
Bujalowski, W., & Jezewska, M. J. (1995) *Biochemistry 34*, 8513−8519.
Bujalowski, W., & Klonowska, M. M. (1993) *Biochemistry 32*, 5888−5900.
Bujalowski, W., & Klonowska, M. M. (1994a) *Biochemistry 33*, 4682−4694.
Bujalowski, W., & Klonowska, M. M. (1994b) *J. Biol. Chem. 269*, 31359−31371.
Bujalowski, W., Klonowska, M. M., & Jezewska, M. J. (1994) *J. Biol. Chem. 269*, 31350−31358.
Bujalowski, W., Lohman, T. M., & Anderson, C. F. (1989) *Biopolymers*, *28*, 1637−1643.
Egelman, E. H., Yu, X., Wild, R., Hingorani, M. M., & Patel, SS. (1995) *Proc. Natl. Acad. Sci. U.S.A. 92*, 3869−3873.
Epstein, I. R. (1978) *Biophys. Chem. 8*, 327−339.
Hill, T. L. (1985) *Cooperativity Theory in Biochemistry*, Springer-Verlag, New York.
Kong, W.-P., Onrust, R., O'Donnell, M., & Kuriyan, J. (1992) *Cell 69*, 425−437.
Kornberg, A., & Baker, T. A. (1992) *DNA Replication*, Freeman, San Francisco.

Kowalczykowski, S. C., Lonberg, N., Newport, J. W., & von Hippel, P. H. (1981) *J. Mol. Biol. 145*, 75−104.
Kubota, Y., Sanjoh, A., Fujisaki, Y., & Steiner, R. F. (1983) *Biophys. Chem. 18*, 233−240.
Lakowicz, J. R. (1983) *Principles of Fluorescence Spectroscopy*, Chapter 10, Plenum Press, New York.
LeBowitz, J. H., & McMacken, R. (1986) *J. Biol. Chem. 261*, 4738−4748.
Ledneva, R. K., Razjivin, A. P., Kost, A. A., & Bogdanov, A. A. (1977) *Nucleic Acids Res. 5*, 4226−4243.
Marians, K. J. (1992) *Annu. Rev. Biochem. 61*, 673−719.
Matson, S. W., & Kaiser-Rogers, K. A. (1990) *Annu. Rev. Biochem. 59*, 289−329.
McGhee, J. D., & von Hippel, P. H. (1974) *J. Mol. Biol. 86*, 469−489.
McMacken, R., Ueda, K., & Kornberg, A. (1977) *J. Biol. Chem. 253*, 3313−3319.
McSwiggen, J. A., Bear, D. G., & von Hippel, P. H. (1988a) *J. Mol. Biol. 199*, 609−622.
Olmsted, M. C., Anderson, C. F., & Record, M. T. (1989) *Proc. Natl. Acad. Sci. U.S.A. 86*, 7766−7770.
Overman, L. B., Bujalowski, W., & and Lohman, T. M. (1988) *Biochemistry 27*, 456−471.
Record, M. T., Lohman, T. M., & deHaseth, P. L. (1976) *J. Mol. Biol. 107*, 145−158.
Reha-Krantz, L. J., & Hurwitz, J. (1978) *J. Biol. Chem. 253*, 4051−4057.
Sambrook, J., Fritsch, E. F., & Maniatis, T. (1989) *Molecular Cloning. A Laboratory Manual*, 2nd ed., Cold Spring Harbor Laboratory Press, Cold Spring Harbor, NY.
San Martin, M. C., Stamford, N. P. J., Dammerova, N., Dixon, N. E., & Carazo, J. M. (1995) *J. Struct. Biol.* (in press).
Secrist, J. A., Bario, J. R., Leonard, N. J., & Weber, G. (1972) *Biochemistry 11*, 3499−3506.
Stasiak, A., Tsaneva, I. R., West, S. C., Benson, C. J. B., Yu, X., & Egelman, E. H. (1993) *Proc. Natl. Acad. Sci. U.S.A. 91*, 7618−7622.
Tanford, C. (1961) *Physical Chemistry of Macromolecules*, J. Wiley, New York.
Tolman, G. L., Barrio, J. R., & Leonard, N. J. (1974) *Biochemistry, 13*, 4869−4878.
Tougu, K., Peng, H., & Marians, K. J. (1994) *J. Biol. Chem. 269*, 4675−4682.
Ueda, K., McMacken, R., & Kornberg, A. (1978) *J. Biol. Chem. 253*, 261−269.
Wahle, E., Lasken, R. S., & Kornberg, A. (1989) *J. Biol. Chem. 264*, 2463−2468.
Wickner, S., Wright, M., & Hurwitz, J. (1973) *Proc. Natl. Acad. Sci. U.S.A. 71*, 783−787.
Williams, K. R., & Konigsberg, W. H. (1991) *Methods Enzymol. 208*, 516−539.

BI952345D